Lamina cribrosa and optic nerve head geometry as a function of myopia in older normal eyes

By

Sara Nourani, O.D.

THESIS

In partial satisfaction of the requirements for the degree of

MASTER OF SCIENCE

in

PHYSIOLOGICAL OPTICS

Presented to the

Graduate Faculty

of the

College of Optometry
University of Houston

August 2017

Approved:

Jason Porter, Ph.D. (Chair)

Ronald Harwerth, O.D., Ph.D.

Danica J Marrelli, O.D.

Lisa Ostrin, O.D., Ph.D.

Acknowledgements

My sincerest thanks to my advisor, Jason Porter, for identifying a potential in me from my very first year in optometry school. I am forever grateful for your guidance to motivate and help open my eyes to the world of research and sacrificing your time to accommodate my hectic schedule. Thank you for always celebrating in my successes and allowing me to learn from my failures with unwavering support. I have learned so much about myself through this process and your mentorship has been invaluable to me, my education, and my career.

Thanks to my family and friends for always supporting me and being my rock through my pursuit of both my masters and doctor of optometry degree. It was always difficult to be away from you during this time but I am who I am today because of you.

Special thanks to the entire Porter lab, to my committee, and the graduate program for working with me and providing support whenever possible.

Lamina cribrosa and optic nerve head geometry as a function of myopia in older normal eyes

By

Sara Nourani, O.D.

THESIS

In partial satisfaction of the requirements for the degree of

MASTER OF SCIENCE

in

PHYSIOLOGICAL OPTICS

Presented to the

Graduate Faculty

of the

College of Optometry
University of Houston

August 2017

Abstract

Purpose: Increased age and levels of myopia are potential risk factors for the development of glaucoma. However, their impact on optic nerve head (ONH) structure in normal eyes has not been fully described. We examined whether differences exist in ONH and lamina cribrosa structure with myopia in older normal eyes.

Methods: Spectral domain optical coherence tomography (SDOCT) scans centered on the ONH were acquired in one eye of 15 older normal subjects (mean = 58.1 ± 7.4 years) with high myopia (spherical equivalent [SE] ≤ -6.00 D) and 16 older normal subjects (mean = 57.5 ± 6.8 years) with emmetropia to moderate myopia (SE = plano to -6.00 D). Retinal nerve fiber layer thickness (RNFLT) was quantified from 12° circular scans. ONH features were marked in each of 48 radial B-scans (20° field) using a semi-automated MATLAB program to calculate Bruch's Membrane Opening (BMO) area and circumference, mean anterior lamina cribrosa surface depth (ALCSD), mean minimum rim width (MRW) and mean scaled MRW.

Results: Refractive errors and axial lengths (ALs) in highly myopic eyes (mean SE = -7.18 ± 1.17 D; mean AL = 26.41 ± 0.76 mm) were statistically different from emmetropic/low myopic eyes (mean SE = -1.59 ± 1.63 D; mean AL = 24.92 ± 1.06 mm) (P<.01). While RNFLT was thinner in older eyes with high myopia (85.5 ± 7.7 µm) compared to those with emmetropia/low myopia (99.2 ± 5.0 µm; P<.01), no significant differences were measured in other ONH parameters between groups. Mean MRW was significantly thinner in highly myopic eyes with larger BMO areas (P=.04) and tended to be thinner in eyes with more posteriorly-located ALCS's (P=.09). Conversely, no

significant relationships were found between MRW and ALCSD (*P*=.60) or BMO area (*P*=.54) in older eyes with emmetropia/low myopia.

Conclusion: The tendency for mean MRW to be thinner in highly myopic eyes with more posteriorly-located ALCS's and larger BMO areas could indicate that axons are pulled toward the BMO in eyes with a deeper lamina. This anatomical configuration may increase the biomechanical susceptibility for glaucomatous axonal damage in older, highly myopic eyes.

Table of Contents

List of Figures

List of Tables

CHAPTER 1

General Introduction

1.1 Introduction

Glaucoma represents a group of optic neuropathies that result in structural changes to the optic nerve head and functional losses in vision (Quigley, 1996), and is currently the leading cause of irreversible blindness worldwide (Pascolini and Mariotti, 2012). Primary open angle glaucoma (POAG), a prevalent type of glaucoma, is known to affect approximately 2 million individuals in the United States (Friedman et al., 2004). It is expected that this number will increase to over 3 million by the year 2020, largely due to an aging population (Friedman et al., 2004). As a chronic condition, glaucoma must be treated and monitored for life as there is no cure. However, the exact mechanism of glaucoma has not yet been fully described. As diagnosis is the first step in preserving vision, it is vital to better understand how eye, optic nerve head (ONH) and vision parameters change in individuals who are at risk for the development of the disease. A better understanding of structural changes in eyes with known risk factors can potentially accelerate proper diagnosis of the disease and help to slow down disease progression and functional vision losses.

The work in this thesis begins by examining whether relationships exist between ONH parameters across older normal eyes. Next, the thesis quantifies relationships between ONH and lamina cribrosa structure in older normal eyes as a function of myopia (a possible risk factor for glaucoma). The thesis concludes with a secondary analysis that determines whether relationships exist in ONH parameters between young and older highly myopic normal eyes (as older age is also a risk factor for glaucoma).

1.2 Myopia

Uncorrected refractive error (myopia) is the single biggest cause of worldwide vision impairment (Naidoo et al., 2014). Myopia, or nearsightedness, affects nearly 30 percent of the North American, European and Australian population. The prevalence of myopia is

even higher in urbanized Asian populations, where an estimated 40-70 percent are affected (Sperduto et al., 1983; Kempen et al., 2005). The prevalence of high myopia, defined by the American Optometric Association as a myopic refractive error greater than 6.00 diopters of sphere (Goss et al., 1997), is prevalent in 1-2 percent of the general population (Sperduto et al., 1983; Li et al., 2009). Due to potentially increasing visual demands in everyday life (e.g., spending considerably more time reading, working at a computer, looking at mobile phones and tablets, or doing other close visual work for long periods of time), the prevalence of myopia and high myopia may also continue to increase. By reason of its rank as the most common of all ocular disorders worldwide and its association with many ocular complications (including glaucoma), myopia remains an important topic of research.

1.2.1 Pathophysiology of myopia

While the exact pathogenesis of myopia remains unclear, there is significant evidence that environmental factors and genetic predispositions likely contribute to the development of myopia. Close working habits, higher levels of education and higher socioeconomic class have all been linked to higher amounts of myopia (Dirani et al., 2008). Moreover, significant evidence shows that people can inherit the tendency to develop myopia, based on studies examining family aggregation trends and twins (Dirani et al., 2006; Hammond et al., 2001). Additionally, 18 linked loci have been identified to have an association with myopia, making its theory of genetic inheritance more viable (Li et al., 2009).

1.2.2 Axial length and myopia

A main structural difference between myopic eyes and hyperopic and emmetropic eyes is its axial length. Myopic eyes tend to have longer axial lengths (Carney et al, 1997;

Grosvenor et al., 1994; Mainstone et al., 1998; Strang et al., 1998; Cheng et al., 1992). Researchers have found the average axial length in an emmetropic eye to be approximately 23.6 mm (Gordon & Donzis, 1985). Based on schematic eyes, one millimeter of axial length growth theoretically corresponds to an approximately 3.00 D increase in myopic refractive error. Studies have also revealed that axial length shows a bimodal distribution in the adult myopic population, with a first peak appearing around an axial length of 24 mm for low to moderate myopia (-6.00 D to plano) and a second peak appearing around 30 mm for high myopia (<-6.00 D) (Tron et al., 1940). Such a distribution likely infers that the physiological mechanisms giving rise to varying levels of myopia may be different, in part explaining why it could be necessary and important to separate low myopia from high myopia in scientific and clinical studies. Although axial length is the primary determinant of refraction, variations in corneal and lens power can also play a role in an eye's refractive error and potentially confound the effects of the degree of myopia on retinal changes due solely to the elongation of the eye.

1.2.3 Clinical presentations associated with high myopia

Posterior fundus changes of the myopic eye are mostly assumed to be a consequence of the axial elongation process that can potentially result in mechanical tissue strain and vascular changes. Optic nerve crescent, lacquer cracks, and posterior staphyloma are among the most common fundus changes found to be associated with increased axial length of the eye (Curtin & Karlin, 1971). Optic nerve crescents can vary in size and location but are typically situated at the temporal disc margin and are a result of the pulling away of the choroid and pigment epithelium. Lacquer cracks are a result of healed linear ruptures in the retinal pigment epithelium and are observed in 4% of high myopes. These disruptions represent a guarded prognosis for vision as they can lead to choroidal neovascular membranes (Klein & Curtin, 1975). Staphylomas result from an

ectasia of the fundus, mostly around the optic nerve head, which can lead to pallor of the area involved. They, too, can be progressive and result in vision loss. Finally, elongation of the eye can cause tilting of the optic disc. In an *en face* view, the optic nerve head appears more vertically oval. This can make for a difficult determination of cup-to-disc ratio and can be detrimental in cases of undiagnosed glaucoma.

1.2.4 ONH structure in high myopia

Previous research has found that the structure of the highly myopic ONH differs from that in eyes with low myopia, emmetropia and hyperopia (Jonas et al., 1988). Normal myopic eyes with longer axial lengths and increased levels of refractive error have been found to have larger optic disc areas (Jonas et al., 1988; Oliveira et al., 2007). Moreover, myopic eyes with longer axial lengths have also been found to have thinner RNFLs and lamina cribrosas (Ren et al., 2009; Malakar et al., 2015).

1.3 Glaucoma and Myopia

1.3.1 Primary Open Angle Glaucoma (POAG)

Primary open angle glaucoma (POAG) is a predominant type of glaucoma that typically occurs in eyes with normal anterior chamber angles (i.e., angles that are not closed or narrow) and elevated intraocular pressure (IOP). POAG results in damage to the optic nerve head and is characterized by an increase in ONH cupping, resulting in a thinning of the neuroretinal rim and visual field losses (Quigley, 1996). Many risk factors have been identified in the development and progression of POAG, including age and high levels of axial myopia (Leske et al., 2003; Perkins and Phelps, 1982; Mitchell et al., 1999; Xu et al., 2007; Quigley, 2011). However, their impact on ONH structure in normal eyes has not yet been fully described.

1.3.2 Myopia as a risk factor for glaucoma

It is unclear whether high levels of myopia predispose the eye to the development of glaucoma and optic neuropathy. The Ocular Hypertension Treatment Study (OHTS) found no significant relationship between myopic refractive error (Spherical Equivalent [SE] of -1.00 D or more) and the risk of developing POAG when grouping all myopic eyes together or when analyzing eyes in subgroups based on their level of myopic refractive error (-1.00 D or less, -1.00 D to -3.00 D, more than -3.00 D) (Gordon et al., 2002). However, several other studies have found a high association between eyes that are myopic and their potential risk for developing POAG. The Barbados Eye Study found myopic refractive error to be a risk factor for open angle glaucoma (Leske et al., 1995). Additionally, the Blue Mountain Eye Study found a 2-3 times higher frequency of glaucoma in myopic eyes compared to non-myopic eyes (Mitchell et al., 1999). Similarly, myopic individuals were 60% more likely to have glaucoma in the Beaver Dam Eye Study, as those with refractive errors of more than -3.00 D had a 3 times higher risk for glaucomatous damage (Wong et al., 2003). The Beijing Eye Study also found the prevalence of glaucomatous optic nerve damage to be higher in patients with highly myopic refractive errors (exceeding -6.00 D) (Xu et al., 2007). Thus, the role of myopic refractive error in the development of glaucoma remains an area for further investigation.

1.4 Optic Nerve Head (ONH) Structure

1.4.1 Retinal Nerve Fiber Layer (RNFL)

The retinal nerve fiber layer (RNFL) is formed by the retinal ganglion cell axons and represents the innermost layer of the fundus. The visual impulses that begin with the rods and cones travel through the ganglion cells and exit the ONH via retinal ganglion cell axons that accumulate in and comprise the RNFL. The thickness of the RNFL increases towards the optic disc in normal eyes, at which point the axons bend and pass

through the scleral canal, forming the neuroretinal rim of the optic nerve head. Visibility of the RNFL decreases with age, with an estimated annual loss of 4,000-5,000 fibers/year (Flanagan and Lonsberry, 2008). The appearance of defects in the RNFL (slit defect, wedge defects) viewed clinically by indirect ophthalmoscopy serves as an important sign for “pre-perimetric” glaucoma, though it is not necessarily pathognomonic of glaucoma. Most often, these defects first occur in the temporal inferior sector and later develop in the temporal superior sector of the ONH in glaucoma (Flanagan and Lonsberry, 2008).

1.4.2 Bruch’s Membrane Opening (BMO)

Bruch’s membrane is the innermost layer of the choroid and is approximately 2-4 μm thick. It is located between the retina and the choroid, extends anteriorly to the ora serrata and is interrupted only by the optic nerve (Curcio & Johnson, 2013). The opening of the optic nerve between the termination points of the retinal pigment epithelium (RPE)/Bruch’s membrane (BM) interface is known as the Bruch’s Membrane Opening (BMO) (see Figs. 2-1, 2-2). Recent studies have demonstrated that the BMO represents the maximum aperture through which retinal ganglion cell axons can pass at the level of the optic nerve head and can be used in metrics that may better detect the onset and change of glaucoma, such as minimum rim width and the depth of the anterior lamina cribrosa surface (Chauhaun et al., 2015).

1.4.3 Minimum Rim Width (MRW)

Minimum rim width (MRW) is the shortest (perpendicular) distance between the RPE/BM termination points and the inner limiting membrane (ILM) (See Fig. 2-3). Mean MRW has recently been proposed as an accurate optical coherence tomography (OCT)-based measurement of the neuroretinal rim. Previous research has shown that mean MRW is

thinner in older normal eyes with low myopia compared to young normal eyes with low myopia (Bhakta et al., 2014). It has also been identified as a potential earlier structural biomarker for glaucomatous disease onset, as changes in mean MRW have been shown to typically precede the earliest changes measured in RNFL thickness, a clinically accepted metric currently used to assess the onset and progression of glaucoma (Strouthidis et al., 2011; He et al., 2014; Patel et al., 2014; Ivers et al., 2015).

1.4.4 Lamina cribrosa

Upon exiting the eye, nerve fiber axons move posteriorly through an opening in the sclera that contains the lamina cribrosa, a three-dimensional tissue composed primarily of dense collagen and elastic fibers that form beams and stretch across the optic nerve as a continuation of the inner sclera. Several studies suggest that damage to retinal ganglion cell axons in glaucoma initially occurs at the lamina cribrosa (Quigley et al., 1981, Burgoyne et al., 2004). Previous research has shown no differences in lamina cribrosa structure between normal young and older eyes with low amounts of myopia (Bhakta et al., 2014). However, the extent to which structural differences in the lamina cribrosa are associated with high refractive errors in older normal eyes (that may be more highly susceptible to glaucomatous optic neuropathy) remains unknown.

1.5 Spectral Domain Optical Coherence Tomography (SDOCT)

Optical Coherence Tomography is a noninvasive technique used to obtain high quality, cross-sectional images of biological tissues in the living eye (Huang et al., 1991). Its recent integration into clinical care has made SDOCT an invaluable tool for clinicians to use in the management of retinal diseases (including glaucoma), primarily due to its ability to provide precise *in vivo* measurements of macular and retinal nerve fiber layer thicknesses, as well as optic nerve structure. SDOCT measurements of retinal and ONH

structure are typically compared against an age-matched normative database. The normative database of the Heidelberg Spectralis SDOCT instrument (used in this study) consists of 201 healthy individuals between the ages of 18 and 78 years. The database is racially homogenous consisting of only Caucasian eyes. Furthermore, all individuals in the normative database are within a range of refractive error between +5.00 D to -7.00 D (Yang et al., 2015). Thus, there is little inclusion of highly myopic eyes in the normative database.

1.6 Specific Aim

The long-term goal of this project is to determine the impact of risk factors for glaucoma (e.g., age, high myopia) on optic nerve head (ONH) and lamina cribrosa structure in normal eyes and eyes with glaucoma. Previous research has shown that most ONH and lamina cribrosa structural parameters are similar between normal young and older eyes with low amounts of myopia (Bhakta et al., 2014). However, the extent to which structural differences in the ONH and lamina cribrosa are associated with the degree of refractive error in older normal eyes that are more highly susceptible to glaucomatous neuropathy has remained relatively unexplored.

We pursued an experiment related to the working hypothesis that normal older highly myopic eyes will exhibit differences in ONH and lamina cribrosa structure (relative to normal older eyes with low myopia) that increase the susceptibility of the normal older, highly myopic eye to the development of POAG. We capitalized on the use of high-resolution spectral domain optical coherence tomography (SDOCT) imaging to test a prediction based on this hypothesis - that normal, older eyes with increasing myopic refractive error will have more posteriorly-located anterior lamina cribrosa surfaces (ALCS's), as the ALCS has been shown to move posteriorly in early stages of glaucoma (Bellezza et al., 2003; Strouthidis et al., 2011; He et al., 2014; Ivers et al., 2015).

SDOCT imaging was used to measure ONH parameters (mean RNFL thickness, BMO area, mean MRW, mean scaled MRW, and mean ALCS depth) in 15 normal human patients (≥ 50 years of age) with spherical equivalent refractive errors of at least -6.00 D. This data was compared with measurements of the same parameters previously acquired in 16 age-matched, normal human subjects with low to moderate degrees of myopia (plano to -6.00 D) (Bhakta et al., 2014). This experiment was expected to reveal whether there were differences in ONH and lamina cribrosa geometry with increasing refractive error (myopia) in normal, older eyes (i.e., eyes with a known risk factor for primary open angle glaucoma). In addition, ONH parameters in 13 normal human patients (<30 years of age) with spherical equivalent refractive errors of at least -6.00 D were measured. We also compared this data with measurements of the same parameters collected in the aforementioned normal older highly myopic human patients as a secondary analysis of differences with age in eyes with high levels of myopia. The following study provides a better understanding of differences in lamina cribrosa and ONH geometry in older normal eyes as a function of refractive error, allowing us to better distinguish between the effects of myopia and the effects of aging plus myopia on laminar and ONH properties. The study also lends potential insights into whether ONH measurements from glaucoma suspects should be compared to age- and refractive error-matched normative data.

CHAPTER 2

Lamina cribrosa and optic nerve head geometry as a function of myopia in older, normal eyes

Contributing Authors

Amitabha S Bhakta, PhD; Danica Marrelli, OD, FAAO; Hope M. Queener; Nimesh B. Patel, OD, PhD, FAAO; Jason Porter, PhD, FAAO

Abstract

Purpose: Increased age and levels of myopia are potential risk factors for the development of glaucoma. However, their impact on optic nerve head (ONH) structure in normal eyes has not been fully described. We examined whether differences exist in ONH and lamina cribrosa structure with myopia in older normal eyes.

Methods: Spectral domain optical coherence tomography (SDOCT) scans (Spectralis SDOCT with Enhanced Depth Imaging) centered on the ONH were acquired in one eye of 15 older normal subjects (mean = 58.1 ± 7.4 years) with high myopia (spherical equivalent [SE] ≤ -6.00 D) and 16 normal subjects (mean = 57.5 ± 6.8 years) with emmetropia to moderate myopia (SE = plano to -6.00 D). Retinal nerve fiber layer thickness (RNFLT) was quantified from 12° circular scans. ONH features (Inner Limiting Membrane, Bruch's Membrane termination points, anterior lamina cribrosa surface [ALCS]) were marked in each of 48 radial B-scans (20° field) using a semi-automated MATLAB program to calculate Bruch's Membrane Opening (BMO) area, mean ALCS depth (ALCSD) and mean minimum rim width (MRW). Dilated refractions were measured (RK600 autorefractor). Ocular biometry was measured (Lenstar) and used to scale SDOCT images to account for differences in retinal magnification.

Results: Refractive errors and axial lengths (ALs) in highly myopic eyes (mean SE = -7.18 ± 1.17 D; mean AL = 26.41 ± 0.76 mm) were statistically different from emmetropic/low myopic eyes (mean SE = -1.59 ± 1.63 D; mean AL = 24.92 ± 1.06 mm) (*P*<.01). While RNFLT was thinner in older normal eyes with high myopia (85.5 ± 7.7 µm) compared to those with emmetropia/low myopia (99.2 ± 5.0 µm; *P*<.01), no significant differences were measured in BMO area, mean ALCSD and mean MRW between groups. Mean MRW was significantly thinner in highly myopic eyes with larger

BMO areas (*P*=.04) and tended to be thinner in eyes with more posteriorly located ALCS's (*P*=.09). Conversely, no significant relationships were found between MRW and ALCSD (*P*=.60) or BMO area (*P*=.54) in older normal eyes with emmetropia/low myopia.

Conclusion: The tendency for mean MRW to be thinner in highly myopic eyes with more posteriorly-located ALCS's and larger BMO areas could indicate that axons are pulled toward the BMO in eyes with a deeper lamina. This anatomical configuration may increase the biomechanical susceptibility for glaucomatous axonal damage in older, highly myopic eyes.

2.1 Introduction

Glaucoma is a group of optic neuropathies that results from damage to retinal ganglion cell axons and the death of retinal ganglion cells (Quigley et al., 1981). This slowly progressing disease is typically characterized clinically by an increase in optic nerve head (ONH) cupping, thinning of the neuroretinal rim and eventual loss of functional vision (Quigley, 1996). However, many clinical parameters used to assess ONH changes in glaucoma are largely subjective in nature (e.g., ONH "cupping," cup-to-disc ratio, vertical disc diameter, neuro-retinal rim thickness, changes in vessel geometry). While retinal nerve fiber layer thickness (RNFLT) is currently a primary, objective metric used clinically to diagnose and assess the progression of glaucoma, recent *in vivo* studies in experimental models of glaucoma have shown that a posterior movement of the anterior lamina cribrosa surface (ALCS) and a thinning of the minimum rim width (MRW) often precede a thinning of the retinal nerve fiber layer (Strouthidis et al., 2011; He et al., 2014; Patel et al., 2014; Ivers et al., 2015). These results suggest that changes in ALCS depth (ALCSD) and/or MRW could be earlier biomarkers for detecting glaucoma compared to RNFLT change. Therefore, there is a need to better understand, characterize, and determine whether relationships exist between these newly described parameters within normal eyes, normal eyes with risk factors for glaucoma, and glaucomatous eyes at different stages of disease.

While multiple risk factors have been identified for the onset and progression of glaucoma (Mitchell et al. 1999; Gordon et al., 2002), their impact on ONH and lamina cribrosa structure in normal eyes has not been fully described. Older age is well established as a primary risk factor for glaucomatous optic neuropathy (Gordon et al., 2002; Leske et al., 2003; Friedman et al., 2004; Tham et al., 2014). In addition, there are conflicting results on whether high levels of myopia may predispose the eye to the onset of glaucoma, with some studies reporting no significant relationship between myopic

refractive error and the risk of developing POAG (e.g., Ocular Hypertension Treatment Study [Gordon et al., 2002]) and multiple other studies reporting a high association between eyes that are myopic and their potential risk for developing glaucoma (e.g., Barbados Eye Study [Leske et al., 1995]; Blue Mountain Eye Study [Mitchell et al., 1999]; Beaver Dam Eye Study [Wong et al., 2003]; Beijing Eye Study [Xu et al., 2007]). Previous research has shown that most ONH and lamina cribrosa structural parameters are similar between normal young and older eyes with low amounts of myopia (Bhakta et al., 2014). However, the extent to which structural differences in the ONH and lamina cribrosa are associated with the degree of refractive error in older normal eyes that are more highly susceptible to glaucoma has remained relatively unexplored.

The primary purpose of this study was to better understand whether differences exist in normal ONH and lamina cribrosa structure with differing levels of myopia in older normal eyes. We measured and examined whether relationships existed between ONH parameters, lamina cribrosa parameters and axial length in older normal eyes before and after separating subjects into emmetropic/low myopic and highly myopic groups. We also performed a secondary analysis to examine the impact of age on ONH structure in high myopes by comparing ONH and lamina cribrosa parameters collected in a group of young normal highly myopic subjects with the same measurements obtained in our aforementioned group of older normal highly myopic eyes. This study provides a better understanding of differences in lamina cribrosa and ONH geometry in older normal eyes as a function of refractive error, allowing us to better distinguish between the effects of myopia and the effects of aging plus myopia on laminar and ONH properties.

2.2 Methods

The study protocol was approved by the Committee for the Protection of Human Subjects at the University of Houston and adhered to the tenets of the Declaration of

Helsinki. Subjects were recruited from the University Eye Institute (at the University of Houston College of Optometry). Informed consent was obtained from all subjects prior to participating in the study. The more myopic eye was selected for examination from 15 normal older human subjects (mean age = 58.1 ± 7.4 years; range = 51-73 years; 9 Caucasian, 3 African American, 2 Asian American, 1 Hispanic American) and 13 normal young human subjects (mean age = 24.4 ± 1.1 years; range = 23-26 years; 8 Caucasian, 5 Asian American) with high myopia (i.e., Spherical Equivalent [SE] refractive errors of at least -6.00 D with no more than -1.50 D of cylinder). Data from these subjects was also compared with data previously collected in our laboratory (Bhakta et al., 2014) in 16 normal older human subjects (mean age = 57.5 ± 6.8 years; range = 50-76 years; 7 Caucasian, 4 Hispanic American, 3 African American, 2 Asian American) with emmetropia to low myopia (SE = plano to -6.00 D) who were recruited with the same inclusion/exclusion criteria and whose data were analyzed using the same methods as in this study. All subjects had best corrected visual acuities of 20/25 or better, clear ocular media (assessed using slit lamp biomicroscopy), intraocular pressures (IOPs) < 21 mmHg (assessed via Goldmann Applanation Tonometry) with no history of elevated IOP, no clinically abnormal/tilted disc features or abnormal retinal nerve fiber layer appearance (assessed using color stereoscopic optic disk photographs), and normal Humphrey visual fields (24–2 Swedish Interactive Threshold Algorithm standard program; False positive and false negative rates < 33%, fixation losses < 20%) with no visual field defects. Subjects with any reported history of ocular disease, retinopathy or amblyopia were excluded from the study. Pupils were dilated with 1.0% tropicamide and 2.5% phenylephrine prior to refraction measurements and ONH imaging using spectral domain optical coherence tomography (SDOCT).

2.2.1 Refraction measurements

The RK600 autorefractor/keratometer (Reichert Technologies) was used to objectively measure the dilated refractive error of each subject. Three repeated measurements were taken and averaged to determine each patient's mean sphere, cylinder and axis. Mean spherocylindrical refractive errors were then converted to spherical equivalent refractive errors (sphere + ½ of the cylinder).

2.2.2 Biometric measurements

The Lenstar (Haag-Streit) was used to measure each subject's axial length, anterior corneal curvature and anterior chamber depth. These biometric data were incorporated into a 4-surface model eye (Li et al., 2010; Ivers et al., 2011) to scale SDOCT images from visual angle to physical retinal size in micrometers for each individual subject.

2.2.3 Spectral domain optical coherence tomography (SDOCT) imaging

The Spectralis HRA+OCT (Heidelberg Engineering) was used to take 12° circular scans centered on the ONH to calculate mean retinal nerve fiber layer thickness (RNFLT). In addition, cross-sectional radial scans (48 B-scans, 20° field size) centered on the ONH were acquired in each eye using Enhanced Depth Imaging. The inner limiting membrane (ILM) was automatically segmented and manually corrected if segmentation errors were noted in all radial B-scans using the Spectralis software. The anterior lamina cribrosa surface (ALCS) and termination points of the Bruch's Membrane (BM)/Retinal Pigment Epithelium (RPE) interface (or Bruch's Membrane Opening [BMO] points) were manually marked in as many B-scans as possible using our laboratory's customized semi-automated MATLAB program (The MathWorks, Inc.) (Fig. 2-1). These delineated features were used to calculate four ONH and lamina cribrosa parameters. BMO area was calculated as the area enclosed by an ellipse best-fit in 3 dimensions to the marked

BMO points (Fig. 2-2a). After fitting a thin plate spline surface to the marked ALCS points (Sredar et al., 2013), we calculated the mean anterior lamina cribrosa surface depth (ALCSD) as the mean perpendicular distance from the BMO plane to the thin plate spline surface contained within the BMO ellipse (Fig. 2-2b). In addition, we calculated mean minimum rim width (MRW) as the average of the minimum distances measured between the marked BMO points and the automatically segmented ILM across as many B-scans as possible (Fig. 2-3). Finally, we computed a scaled version of MRW for each eye using the method described by Patel et al. (2014) to account for differences in optic disc size across subjects. Scaled MRW (sMRW) was calculated by multiplying an eye's mean MRW by the ratio of its BMO circumference to the mean BMO circumference of a normal population (4,825 μm) (Patel et al., 2014):

$$sMRW\ (\mu m) = MRW(\mu m) * \frac{BMO\ Circumference\ (individual\ eye)}{Mean\ BMO\ Circumference\ of\ Population} \quad (1)$$

$$= MRW(\mu m) * \frac{BMO\ Circumference\ (individual\ eye)}{4{,}825\ \mu m} \quad (2)$$

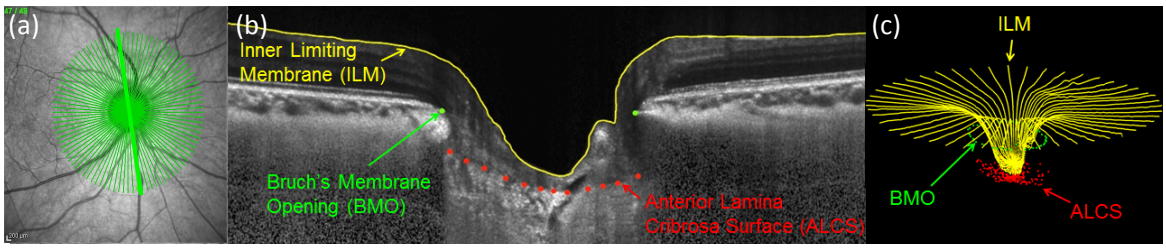

Figure 2-1. SDOCT imaging and delineation of ONH and lamina cribrosa features. (a) En face scanning laser ophthalmoscope image of the ONH showing the locations of all 48 radial B-Scans (green lines) acquired using the Spectralis HRA+OCT. (b) Single radial B-scan of the ONH corresponding to the bold green line in (a) that depicts the automatically segmented Inner Limiting Membrane (ILM, yellow line) and manually marked locations of the Bruch's Membrane Opening (BMO, green points) and Anterior Lamina Cribrosa Surface (ALCS, red points). (c) A three-dimensional point cloud illustrating the ILM, BMO and ALCS markings made in as many radial B-scans as possible.

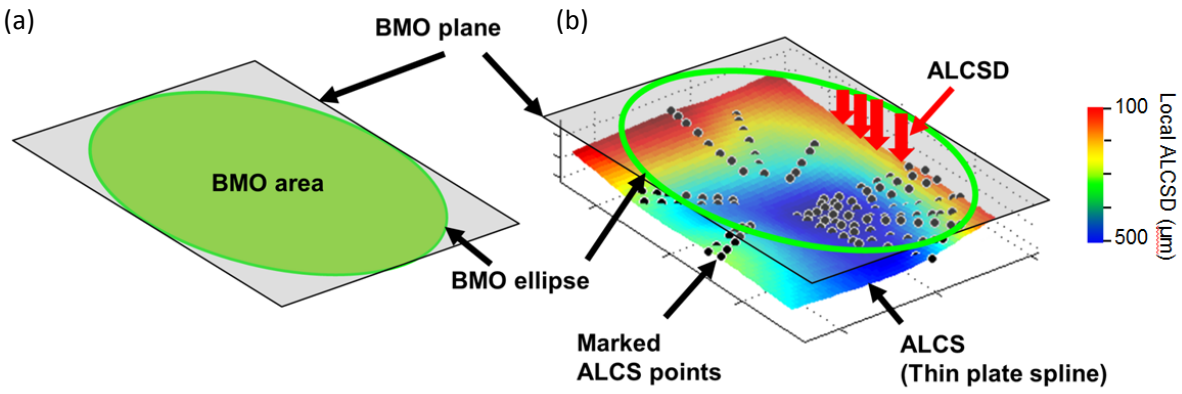

Figure 2-2. Calculation of BMO area and mean ALCSD from delineated SDOCT images. (a) An ellipse (bold, green line) was best-fit in 3-dimensions to the marked BMO points and used to define a BMO plane (gray). BMO area was calculated as the area enclosed by the BMO ellipse on the BMO plane. (b) A thin plate spline was fit to the marked ALCS points (black dots that reside above and below the fitted surface). The perpendicular distance from the BMO plane to each point on the thin plate spline was computed as the local ALCSD (individual red arrows, whose depth is given by the color scale on the right). Mean ALCSD was calculated as the average of all local ALCSD's within the BMO ellipse.

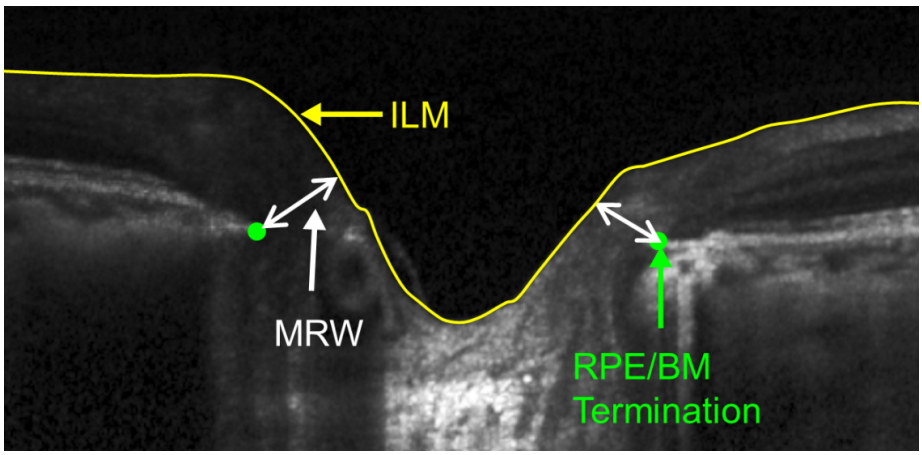

Figure 2-3. Calculation of mean minimum rim width (MRW). Mean MRW was calculated as the mean of the minimum (perpendicular) distances (white lines) measured between the marked BMO points (green dots) and the ILM (yellow line) across all radial B-scans.

2.2.4 Statistical analyses

Statistical analyses were performed using SigmaPlot (Systat Software Inc.), a commercially available software program. The Mann-Whitney rank sum test was used to compare and assess whether statistically significant differences existed in SDOCT-derived parameters between (1) older normal eyes with high myopia and older normal eyes with emmetropia/low myopia, as well as between (2) young and older normal eyes with high myopia. *P* values <.05 represented statistically significant differences between comparisons. Linear regression analyses were also performed between axial length, ONH and laminar parameters for all 3 groups. Corrections for multiple comparisons were made using the Benjamini Hochberg method using a false discovery rate of 5%. Adjusted *P* values <.05 represented statistically significant relationships between the parameters being analyzed.

2.3 Results

2.3.1 Older normal eyes

The degree of relationship between ONH / lamina cribrosa parameters and axial length was examined across all 31 older normal eyes (Fig. 2-4). After correcting for multiple comparisons, no statistically significant relationships were found between BMO area, mean ALCSD, mean MRW or mean sMRW and axial length (*P*>.05) in these subjects (Fig. 2-4a-d). However, consistent with previous studies, mean RNFLT was significantly correlated with axial length (Fig. 2-4e). Older normal eyes with longer axial lengths tended to have thinner RNFLs (*P*=.006).

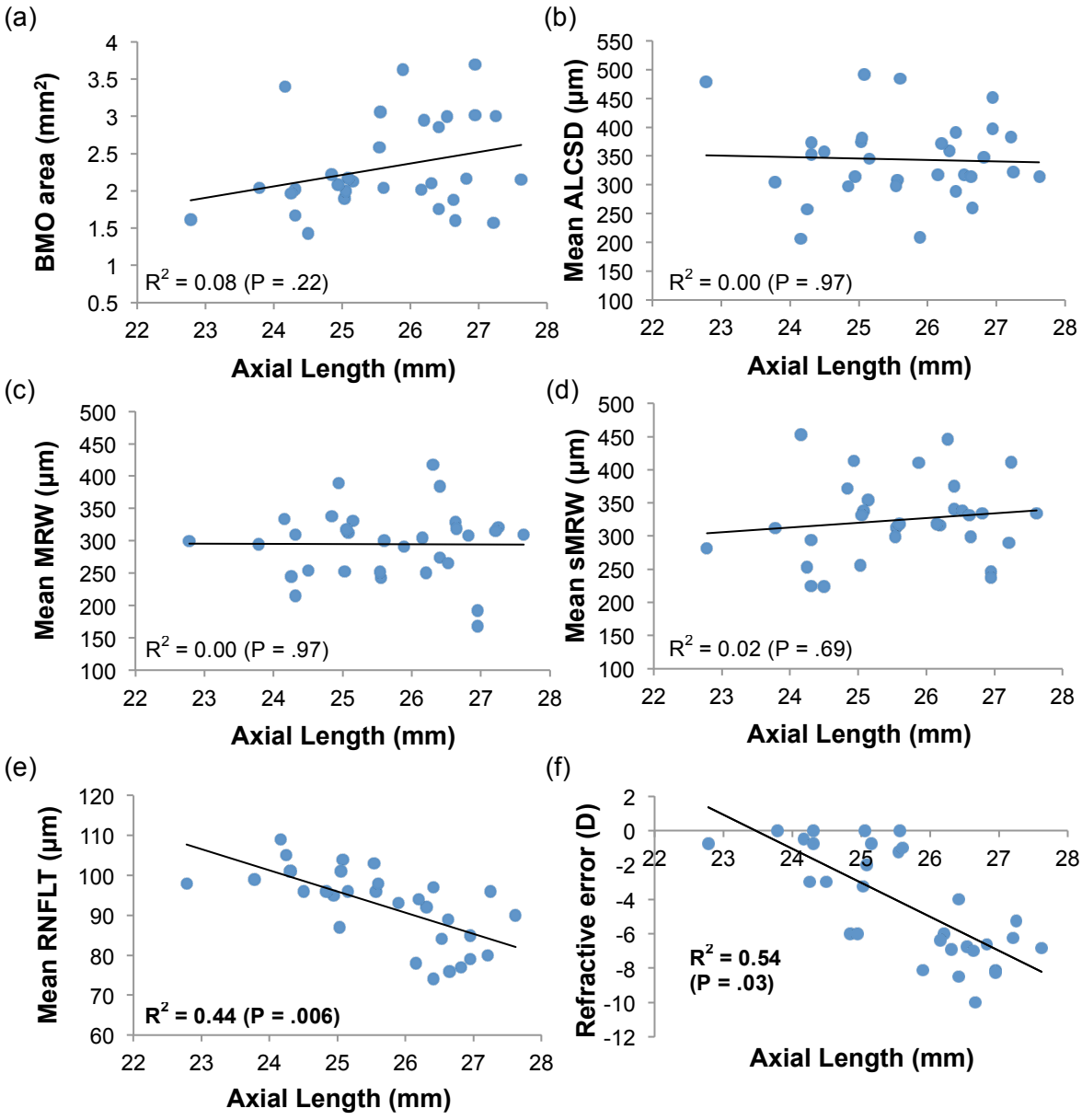

Figure 2-4. Comparison of ONH and refractive parameters plotted as a function of axial length across all older normal eyes. Solid lines indicate linear regressions fit to the corresponding data points. P values were adjusted for multiple comparisons. No significant relationships were seen between (a) BMO area, (b) mean ALCSD, (c) mean MRW or (d) mean sMRW and axial length in older normal eyes. (e) However, mean RNFLT was significantly thinner in older normal eyes with longer axial lengths. (f) There was a significant correlation between spherical equivalent refractive error and axial length across all older normal eyes.

Figures 2-5 through 2-7 summarize the degrees of relationship found between ONH / lamina cribrosa parameters in all older normal eyes. While not statistically significant (*P*=.12), there was a trend for mean MRW to decrease (be thinner) in older normal eyes with larger BMO areas (Fig. 2-5b). There were also no significant correlations between other measured ONH parameters, including mean ALCSD (Fig. 2-5a), mean sMRW (Fig. 2-5c) and mean RNFLT (Fig. 2-5d) and BMO area in older normal eyes.

When examining the extent of relationships between axon-related ONH parameters and mean ALCSD, no significant correlation was found between mean MRW and mean ALCSD (Fig. 2-6a). Once scaled, mean sMRW tended to decrease (become thinner) in older normal eyes with increasing mean ALCSDs (more posteriorly-located ALCS's) (Figure 2-6b). However, this result was not statistically significant after correcting for multiple comparisons (*P*=.09). As shown in Fig. 2-6c, there was no significant correlation between mean RNFLT and mean ALCSD (*P* =.96).

Our examination of axon-related ONH parameters revealed an expected, significant relationship between mean sMRW and mean MRW across all older normal eyes (Fig. 2-7a). However, no statistically significant relationships were observed between mean RNFLT and mean MRW (Fig. 2-7b) or between mean RNFLT and mean sMRW (Fig. 2-7c) across all older normal eyes.

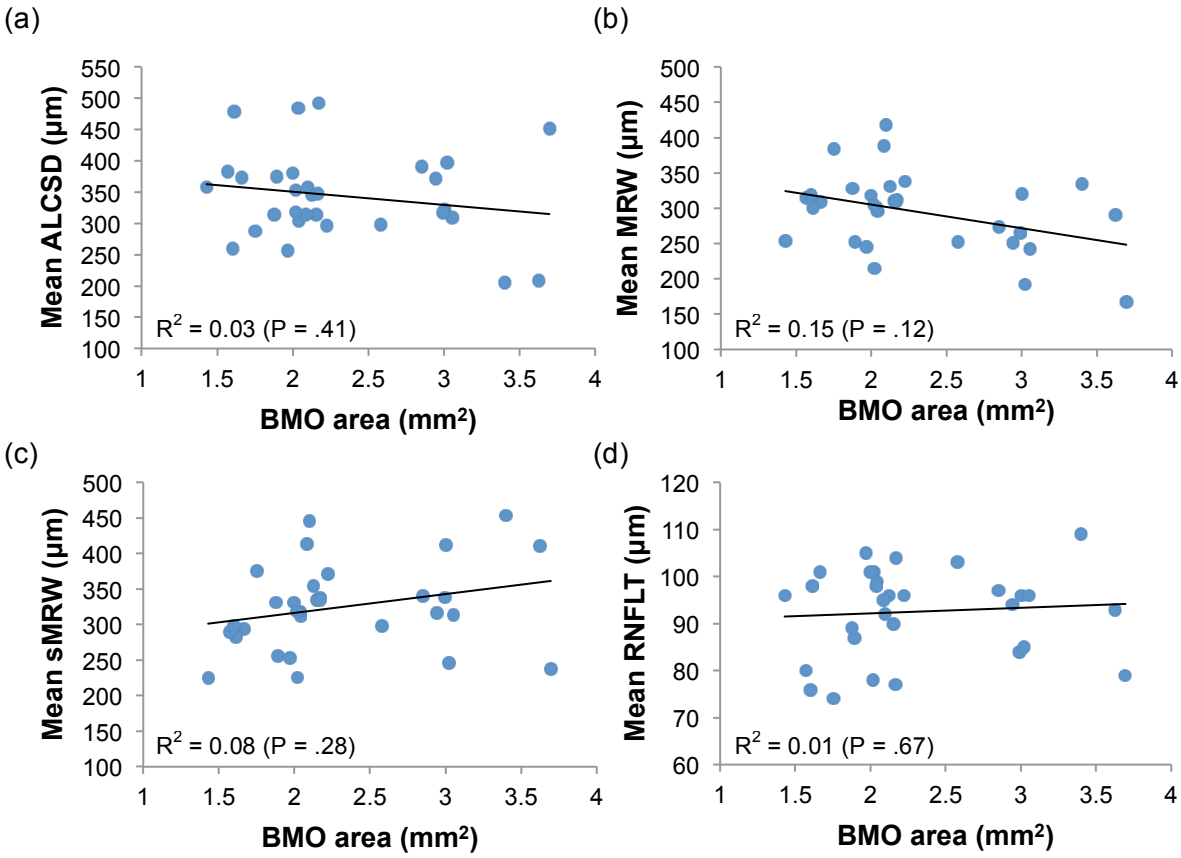

Figure 2-5. Comparison of ONH parameters plotted as a function of BMO area across all older normal eyes. Solid lines indicate linear regressions fit to the corresponding data points. P values were adjusted for multiple comparisons. There were no significant relationships between (a) mean ALCSD, (b) mean MRW, (c) mean sMRW or (d) mean RNFLT and BMO area in older normal eyes.

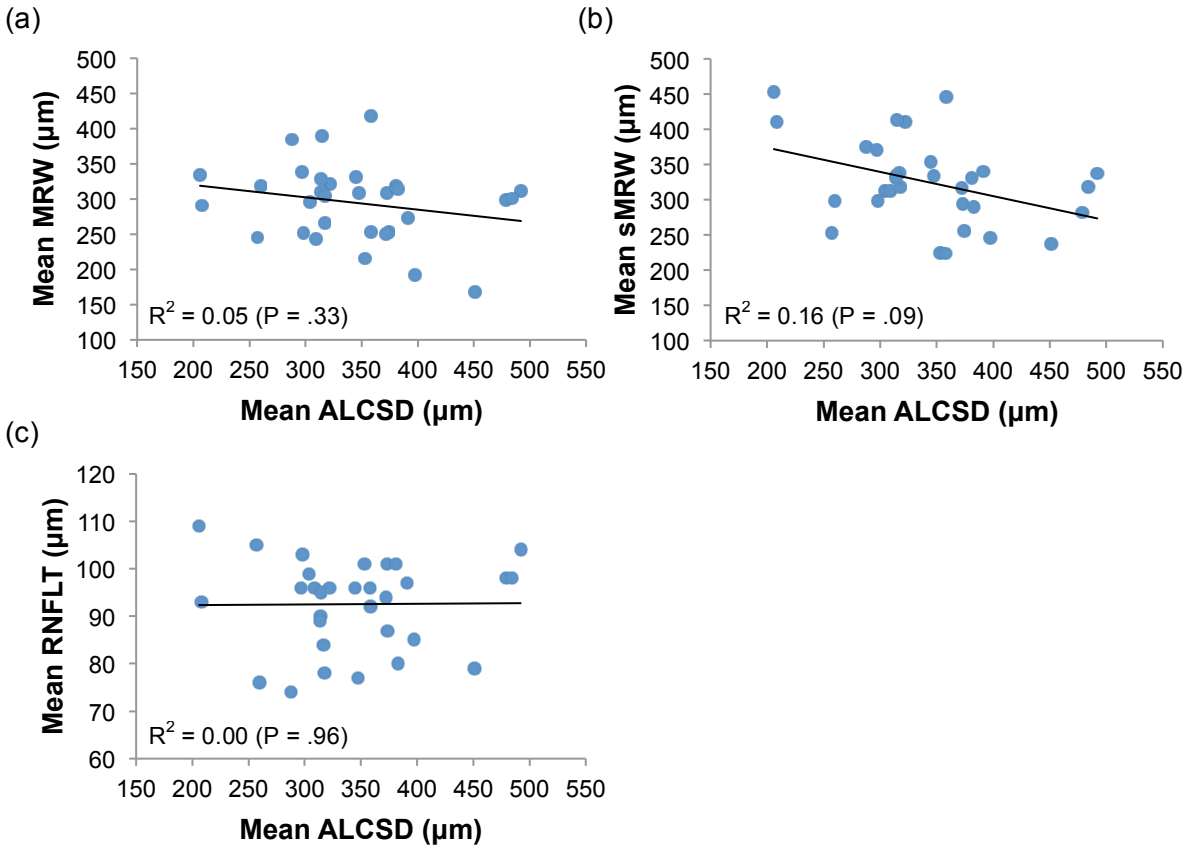

Figure 2-6. Comparison of ONH parameters plotted as a function of mean ALCSD across all older normal eyes. Solid lines indicate linear regressions fit to corresponding data points. P values were adjusted for multiple comparisons. (a) There was no correlation between mean MRW and mean ALCSD in older normal eyes. (b) Mean sMRW tended to be thinner in older normal eyes with increased mean ALCSDs (i.e., more posteriorly-located ALCS's), but this trend did not reach significance (*P*=.09). (c) No relationship was found between mean RNFLT and mean ALCSD in older normal eyes.

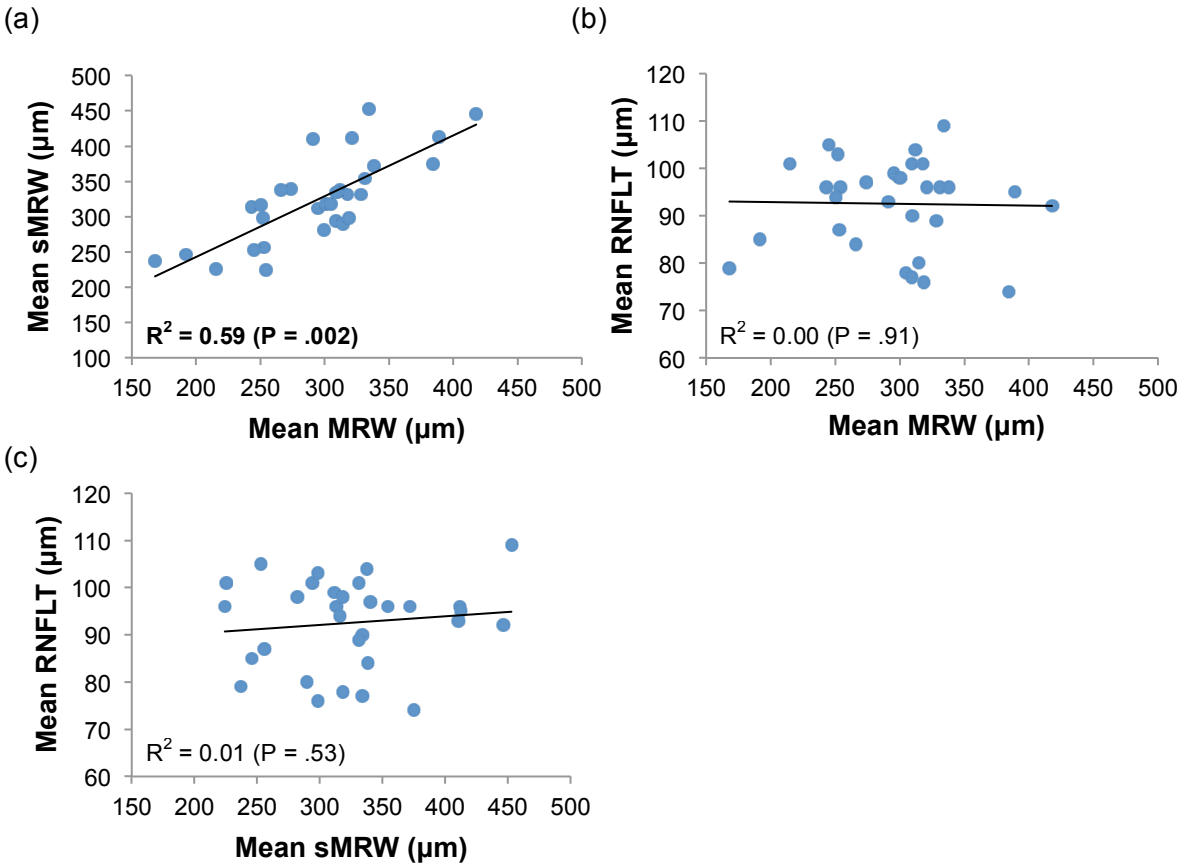

Figure 2-7. Comparison of ONH parameters plotted as a function of (a,b) mean MRW and (c) mean sMRW across all older normal eyes. Solid lines indicate linear regressions fit to corresponding data points. P values were adjusted for multiple comparisons. (a) Mean sMRW was significantly correlated with mean MRW in older normal eyes. However, there were no significant relationships between (b) mean RNFLT and mean MRW or between (c) mean RNFLT and mean sMRW in older normal eyes.

2.3.2 Older emmetropes/low myopes vs older high myopes

The majority of measured ONH and lamina cribrosa parameters were not significantly different between 16 older normal eyes with emmetropia/low myopia (mean SE = -1.59 ± 1.63 D) and 15 older normal eyes with high myopia (mean SE = -7.18 ± 1.17 D) (Table 2-1). Mean RNFLT was the only measured ONH parameter found to be significantly different between groups (P<.01), as older high myopes had thinner mean RNFLTs (85.5 ± 7.7 μm) compared to the older emmetropes/low myopes (99.2 ± 5.0 μm).

We examined whether relationships existed between measured ONH / lamina cribrosa parameters and axial length in older eyes with emmetropia/low myopia and in those with high myopia (Fig. 2-8). While not statistically significant (P=.09), BMO area tended to increase with axial length in older emmetropes/low mopes (Fig. 2-8a), indicating that older emmetropic/low myopic eyes with longer eyes tended to have larger BMO areas. However, no statistically significant relationships were found between any other examined ONH parameters and axial length in older emmetropic/low myopic eyes (Fig. 2-8b-f). In older highly myopic eyes, there were no significant relationships between BMO area and axial length (Fig. 2-8a), or between any other ONH parameter and axial length (Fig. 2-8b-f).

Table 2-1: Mean measures of age, spherical equivalent refractive error, axial length and ONH parameters across older emmetropic/low myopic and highly myopic subjects.

	Older Emmetropes/ Low Myopes (N = 16)	Older High Myopes (N = 15)	Mann-Whitney (*P-value*)
	Mean ± SD (Range)	**Mean ± SD (Range)**	
Age (years)	57.5 ± 6.8 (50 - 76)	58.1 ± 7.4 (51 - 73)	*P* = .83
Spherical Equivalent (D)	-1.59 ± 1.63 (Plano - -4.00)	-7.18 ± 1.17 (-6.00 - -10.25)	*P* < .01
Axial Length (mm)	24.92 ± 1.06 (22.78 - 26.41)	26.41 ± 0.76 (24.84 - 27.62)	*P* < .01
BMO Area (mm^2)	2.240 ± 0.569 (1.429 - 3.400)	2.388 ± 0.693 (1.571 - 3.696)	*P* = .57
Mean ALCSD (µm)	357.9 ± 79.3 (206.3 - 334.0)	329.2 ± 58.9 (208.3 - 451.2)	*P* = .33
Mean MRW (µm)	284.8 ± 36.7 (243.0 - 334.0)	305.4 ± 67.8 (168.0 - 417.8)	*P* = .24
Scaled MRW (µm)	312.7 ± 61.4 (224.2 - 452.8)	337.2 ± 58.9 (237.2 - 446.1)	*P* = .23
Mean RNFLT (µm)	99.2 ± 5.0 (87 - 109)	85.5 ± 7.7 (74 - 96)	*P* < 0.01

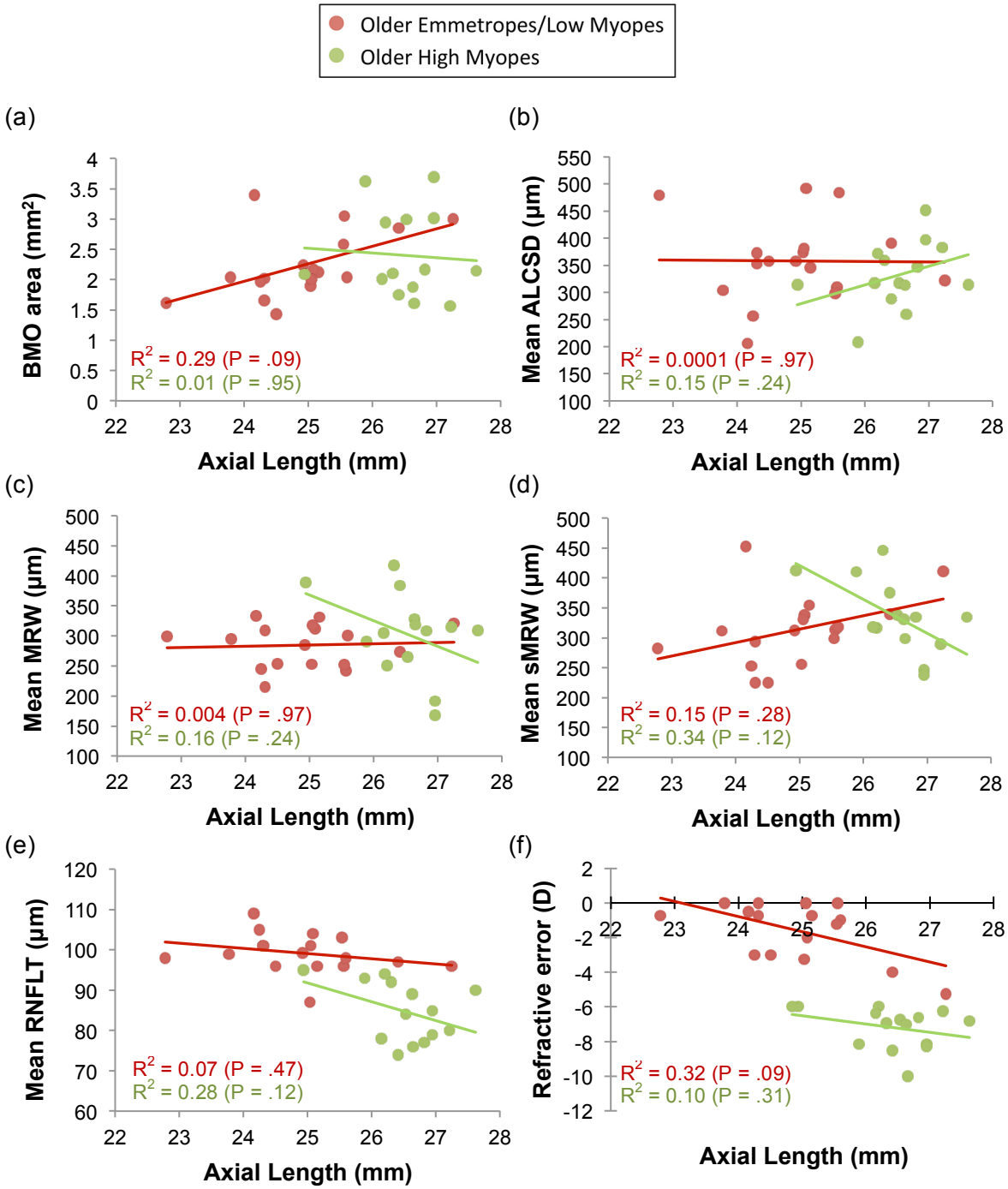

Figure 2-8. Comparison of ONH and refractive parameters plotted as a function of axial length between older normal eyes with emmetropia/low myopia (red circles) and older normal eyes with high myopia (green circles). Solid lines indicate linear regressions fit to the corresponding data points. P values were adjusted for multiple comparisons. (a) While not significant, BMO area tended to be larger in older emmetropic/low myopic eyes with longer axial lengths. No significant relationships were found between (b) mean

ALCSD, (c) mean MRW, (d) mean sMRW, (e) mean RNFLT or (f) Refractive error and axial length in older emmetropic/low myopic eyes or older highly myopic eyes.

We also investigated whether correlations existed between ONH / lamina cribrosa parameters within older emmetropic/low myopic and highly myopic groups (Fig. 2-9). No statistically significant relationships were found between mean ALCSD and BMO area (Fig. 2-9a) or between mean RNFLT and BMO area (Fig. 2-9d) within either group of eyes, despite a tendency for the ALCS to be more anteriorly located (i.e., decreased mean ALCSD) in older emmetropic/low myopic eyes with larger BMO areas (*P*=.10) (Fig. 2-9a). While no significant linear relationship was found between mean MRW and BMO area in older emmetropic/low myopic eyes (Fig. 2-9b), mean sMRW significantly increased (was thicker) in older emmetropic/low myopic eyes with larger BMO areas (Fig. 2-9c). However, statistically significant relationships were found in an opposite fashion in older highly myopic eyes. Mean MRW significantly decreased (was thinner) in older high myopes with larger BMO areas (Fig. 2-9b), while no significant relationship was found between mean sMRW and BMO area (Fig. 2-9c) in the same group of eyes.

There were no significant relationships between any axon-related parameters (mean MRW, sMRW or RNFLT) and mean ALCSD in older eyes with emmetropia/low myopia (Fig. 2-10). While not significant, a trend was observed between mean MRW and mean ALCSD in older eyes with high myopia (Fig. 2-10a), suggesting that eyes with more posteriorly-located ALCS's had thinner MRWs. After scaling MRW for each eye's individual BMO size, mean sMRW tended to decrease (be thinner) in older high myopes with larger mean ALCSDs (deeper ALCS's) (*P*=.06) (Fig. 2-10b). There was no significant relationship between mean RNFLT and mean ALCSD for either group (Fig. 2-10c).

Similar relationships were found when comparing axon-related parameters in older emmetropic/low myopic and highly myopic eyes. As expected, mean sMRW was strongly and positively correlated with mean MRW in both groups (Fig. 2-11a). However,

mean RNFLT was not significantly correlated with mean MRW (Fig. 2-11b) or mean sMRW (Fig. 2-11c) in either group.

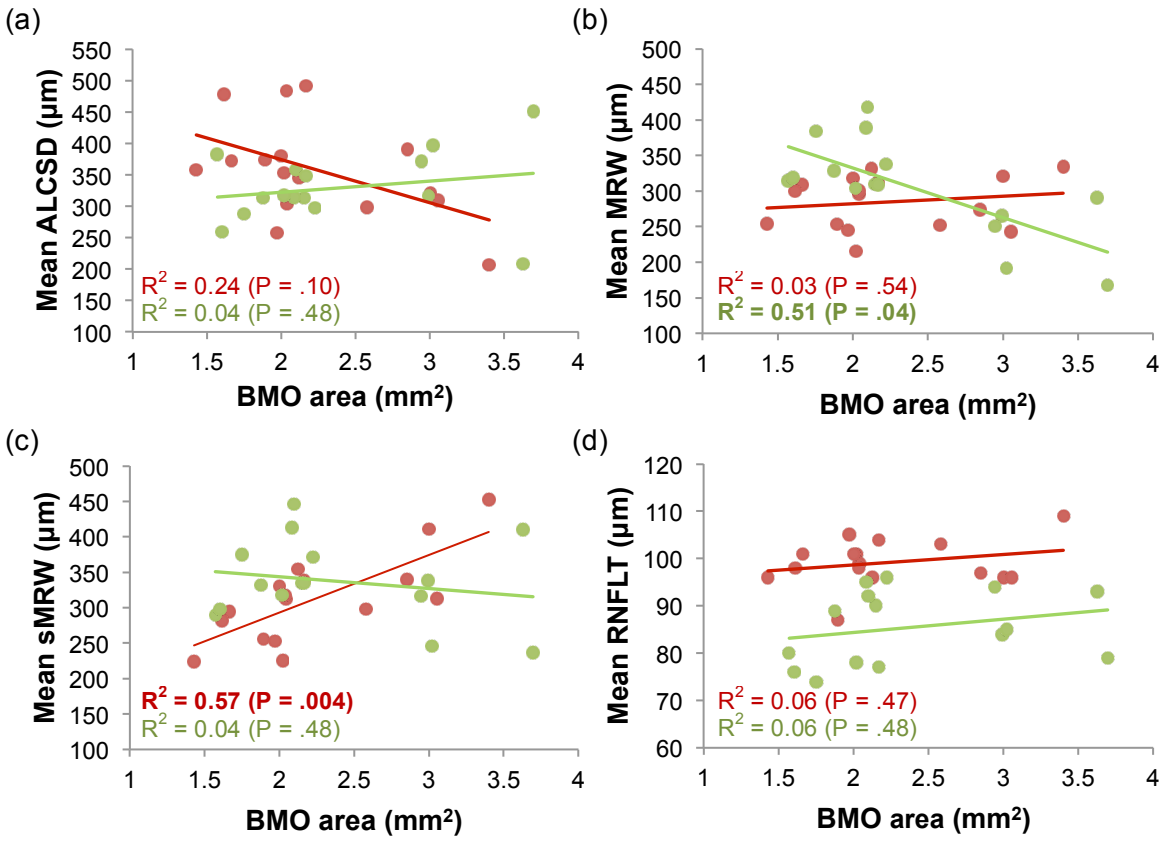

Figure 2-9. Comparison of ONH parameters plotted as a function of BMO area between older normal eyes with emmetropia/low myopia (red circles) and older normal eyes with high myopia (green circles). Solid lines indicate linear regressions fit to the corresponding data points. P values were adjusted for multiple comparisons. (a) While not significant (*P*=.10), mean ALCSD tended to decrease (i.e., the ALCS tended to be more anteriorly-located) only in older emmetropic/low myopic eyes with larger BMO areas. (b) Mean MRW was significantly thinner in older highly myopic eyes with larger BMO areas, but not in older emmetropic/low myopic eyes. (c) Mean sMRW was significantly thicker only in older emmetropic/low myopic eyes with larger BMO areas. (d) No significant relationships were measured between mean RNFLT and BMO area in older emmetropic/low myopic or highly myopic eyes.

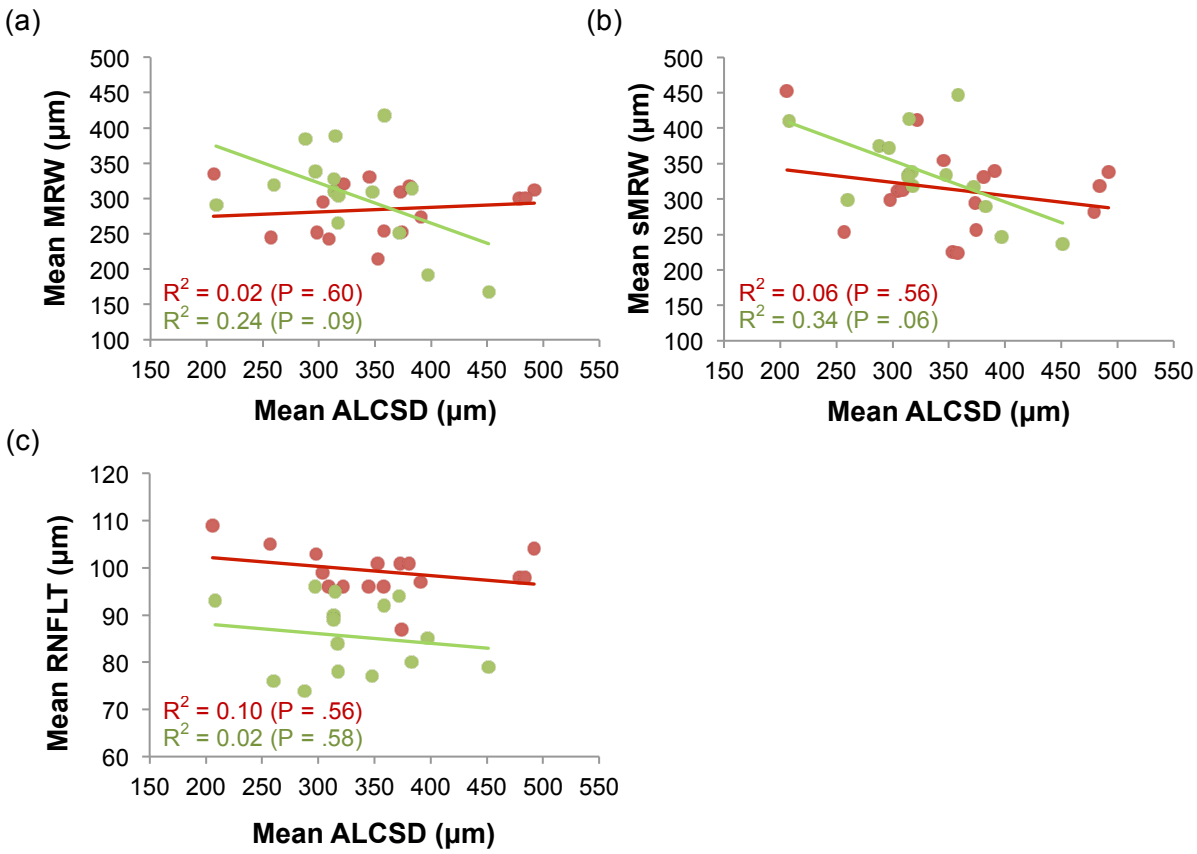

Figure 2-10. Comparison of ONH parameters plotted as a function of mean ALCSD between older normal eyes with emmetropia/low myopia (red circles) and older normal eyes with high myopia (green circles). Solid lines indicate linear regressions fit to the corresponding data points. P values were adjusted for multiple comparisons. (a) There were no statistically significant relationships between mean MRW and mean ALCSD in older emmetropic/low myopic or highly myopic eyes. (b) While not significant (*P*=.06), mean sMRW tended to be thinner in older highly myopic eyes with increased mean ALCSDs (i.e., more posteriorly-located ALCS's). (c) No relationships were found between mean RNFLT and mean ALCSD in older emmetropic/low myopic or highly myopic eyes.

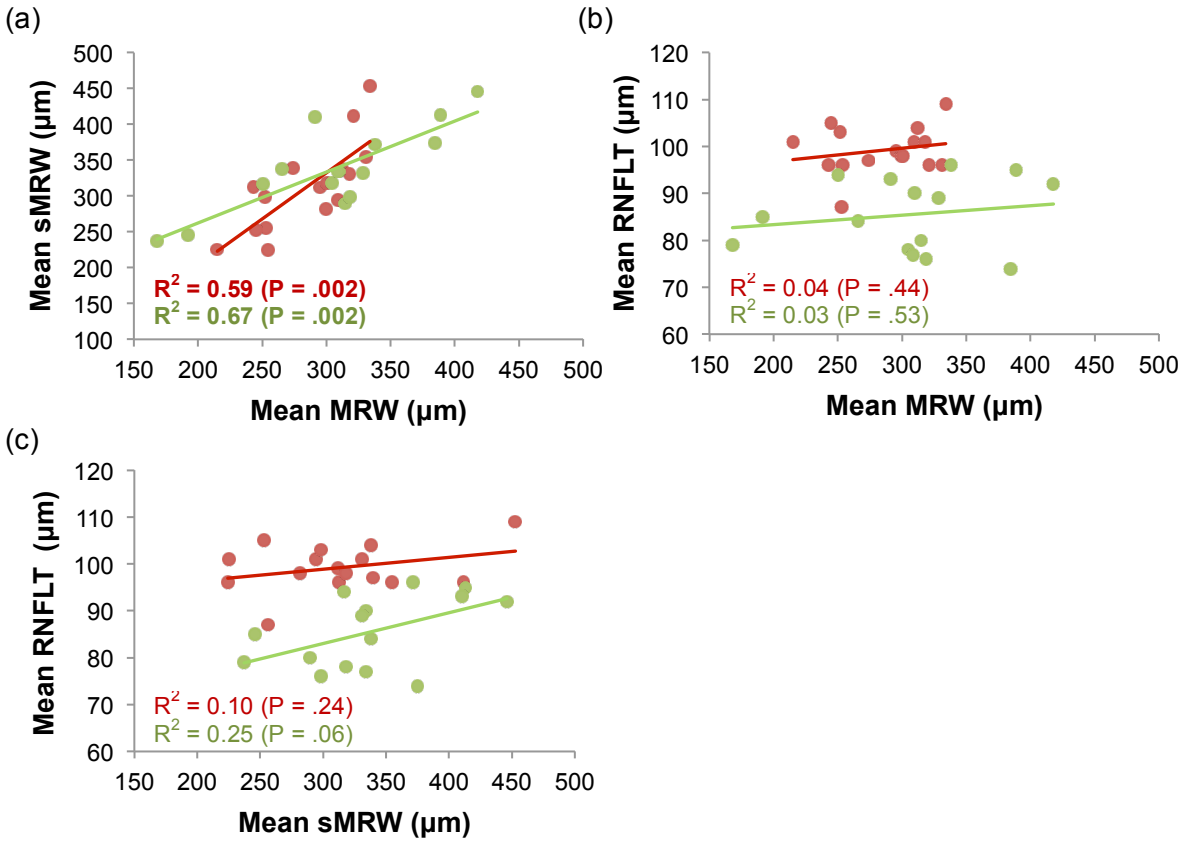

Figure 2-11. Comparison of ONH parameters plotted as a function of (a,b) mean MRW and (c) mean sMRW between older normal eyes with emmetropia/low myopia (red circles) and older normal eyes with high myopia (green circles). Solid lines indicate linear regressions fit to the corresponding data points. P values were adjusted for multiple comparisons. (a) Mean sMRW was significantly correlated with mean MRW in older emmetropic/low myopic and highly myopic eyes. However, there were no significant relationships between (b) mean RNFLT and mean MRW or between (c) mean RNFLT and mean sMRW in older emmetropic/low myopic or highly myopic eyes.

2.3.3 Young high myopes vs older high myopes

As shown in Table 2-2, spherical equivalent refractive error and axial length were similar between our 13 normal young eyes with high myopia (mean SE = -7.71 ± 1.52 D) and our 15 normal older eyes with high myopia (mean SE = -7.18 ± 1.17 D). While some ONH and laminar parameters were also similar between these two groups (e.g., BMO area, mean ALCSD), all axon-related ONH parameters (i.e., mean MRW, mean sMRW and mean RNFLT) were significantly different between young and older highly myopic eyes ($P \leq .02$).

The degree of relationship between all ONH / lamina cribrosa parameters and axial length was again examined, this time for young and older highly myopic eyes (Figure 2-12). In general, the young high myopes demonstrated similar trends as the older emmetropes/low myopes (presented in Fig. 2-8). BMO area was the only analyzed parameter that was significantly correlated with axial length in young highly myopic eyes (Figure 2-12a). Young high myopes with longer axial lengths tended to have larger BMO areas ($P < .001$). As shown earlier (Fig. 2-8), no ONH parameters were significantly correlated with axial length in older highly myopic eyes.

Table 2-2: Mean measures of age, spherical equivalent refractive error, axial length and ONH parameters across young and older highly myopic eyes**.**

	Young High Myopes (N = 13)	Older High Myopes (N = 15)	Mann-Whitney (*P-value*)
	Mean ± SD (Range)	**Mean ± SD (Range)**	
Age (years)	24.4 ± 1.1 (23 - 26)	58.1 ± 7.4 (51 - 73)	*P* < 0.01
Spherical Equivalent (D)	-7.71 ± 1.52 (-6.00 - -10.75)	-7.18 ± 1.17 (-6.00 - -10.25)	*P* = .41
Axial Length (mm)	26.18 ± 0.94 (24.82 - 27.78)	26.41 ± 0.76 (24.84 - 27.62)	*P* = .41
BMO Area (mm^2)	2.179 ± 0.433 (1.412 - 2.858)	2.388 ± 0.693 (1.571 - 3.696)	*P* = .68
Mean ALCSD (µm)	298.1 ± 50.9 (213.2 - 399.1)	329.2 ± 58.9 (208.3 - 451.2)	*P* = .20
Mean MRW (µm)	369.6 ± 48.4 (248.1 - 430.7)	305.4 ± 67.8 (168.0 - 417.8)	*P* = .01
Scaled MRW (µm)	398.7 ± 55.2 (307.1 - 477.2)	337.2 ± 58.9 (237.2 - 446.1)	*P* = .01
Mean RNFLT (µm)	94.0 ± 9.7 (81 - 111)	85.5 ± 7.7 (74 - 96)	*P* = .02

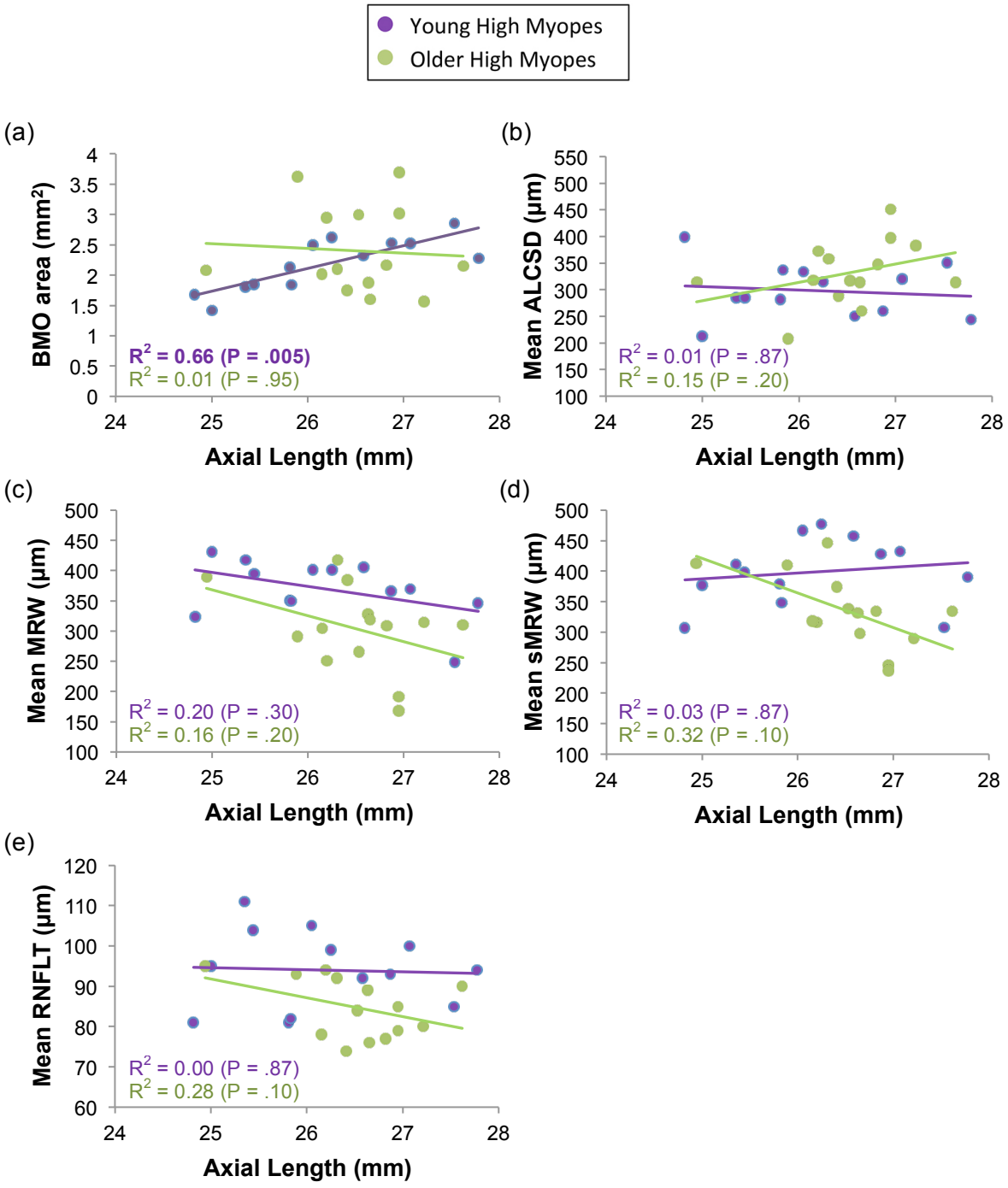

Figure 2-12. Comparison of ONH parameters plotted as a function of axial length between young normal eyes with high myopia (purple circles) and older normal eyes with high myopia (green circles). Solid lines indicate linear regressions fit to the corresponding data points. P values were adjusted for multiple comparisons. (a) BMO area significantly increased in young highly myopic eyes with longer axial lengths, but not in older highly myopic eyes. No significant relationships were seen between

(b) mean ALCSD and axial length or between (c) mean MRW and axial length in young or older highly myopic groups. While not statistically significant, (d) mean sMRW and (e) mean RNFLT tended to be thinner in older highly myopic eyes with longer axial lengths (*P*=.10), but not in young high myopes.

Comparisons were again made between ONH / lamina cribrosa parameters in both groups. No statistically significant linear relationships were found between mean ALCSD (Fig. 2-13a), mean sMRW (Fig. 2-13c) or mean RNFLT (Fig. 2-13d) and BMO area (P>.05) in young or older highly myopic eyes. Mean MRW significantly decreased (became thinner) in older highly myopic eyes with larger BMO areas (P=.04; Fig. 2-13b). However the same relationship was not observed in the young highly myopic eyes (P=.48).

The trends observed between axon-related ONH parameters and mean ALCSD were similar between young and older highly myopic eyes (Fig. 2-14). While not statistically significant, there was a tendency for mean MRW to be thinner (decreased mean MRW) in young and older highly myopic eyes with more posteriorly-located ALCS's (increased mean ALCSDs) (Fig. 2-14a). After scaling, the relationship between sMRW and mean ALCSD were nearly significant only in the older highly myopic eyes (P=.06; Fig. 2-14b). No statistically significant relationships were found between mean RNFLT and mean ALCSD in either population (Fig. 2-14c).

When comparing axon-related ONH parameters, there were again significant and expected correlations between mean sMRW and mean MRW in both groups (Fig. 2-15a). Mean RNFLT was significantly thicker in young highly myopic eyes with thicker mean MRWs (Fig. 2-15b) and mean sMRWs (Fig. 2-15c). However, the same relationships were not found in the older highly myopic eyes, despite a tendency for mean RNFLT to be larger in older highly myopic eyes with larger mean sMRWs (P=.06) (Fig. 2-15c).

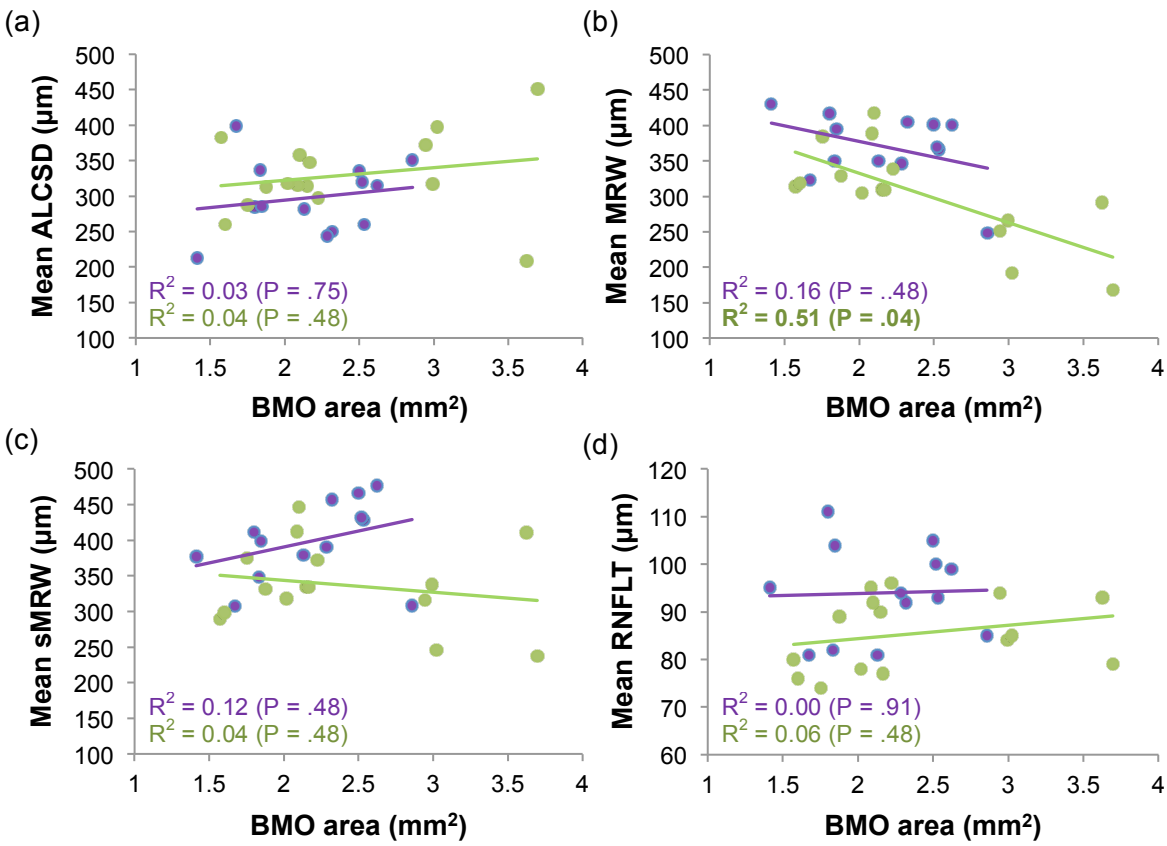

Figure 2-13. Comparison of ONH parameters plotted as a function of BMO area between young normal eyes with high myopia (purple circles) and older normal eyes with high myopia (green circles). Solid lines indicate linear regressions fit to the corresponding data points. P values were adjusted for multiple comparisons. (a) There was no correlation between mean ALCSD and BMO area in young or older highly myopic eyes. (b) Mean MRW was significantly thinner in older highly myopic eyes with larger BMO areas, but not in young highly myopic eyes. No significant relationships were measured between (c) mean sMRW and BMO area or between (d) mean RNFLT and BMO area in young or older highly myopic eyes.

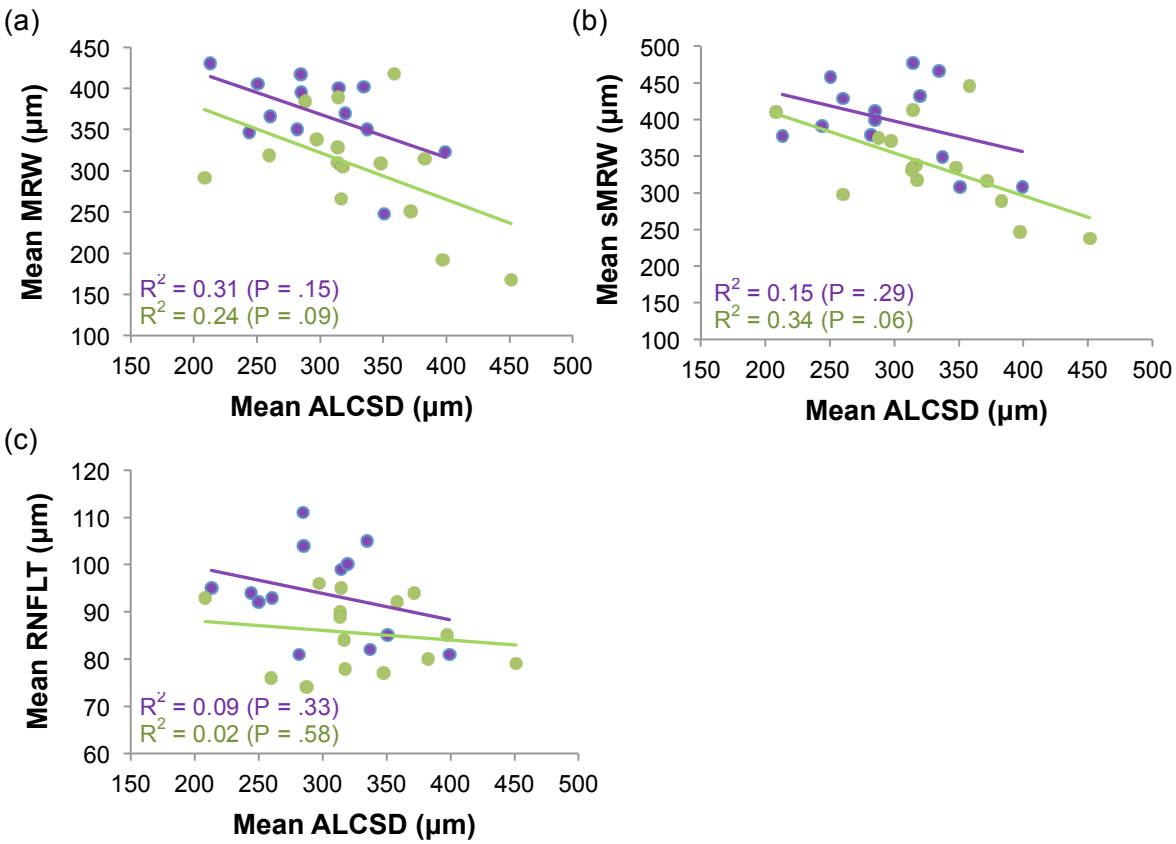

Figure 2-14. Comparison of ONH parameters plotted as a function of mean ALCSD between young normal eyes with high myopia (purple circles) and older normal eyes with high myopia (green circles). Solid lines indicate linear regressions fit to the corresponding data points. P values were adjusted for multiple comparisons. (a) There was a trend for mean MRW to be thinner in older highly myopic eyes with increased mean ALCSDs (i.e., more posteriorly-located ALCS's). (b) While not significant, mean sMRW tended to be thinner in older highly myopic eyes with increased mean ALCSDs. (c) No relationships were found between mean RNFLT and mean ALCSD in young or older highly myopic eyes.

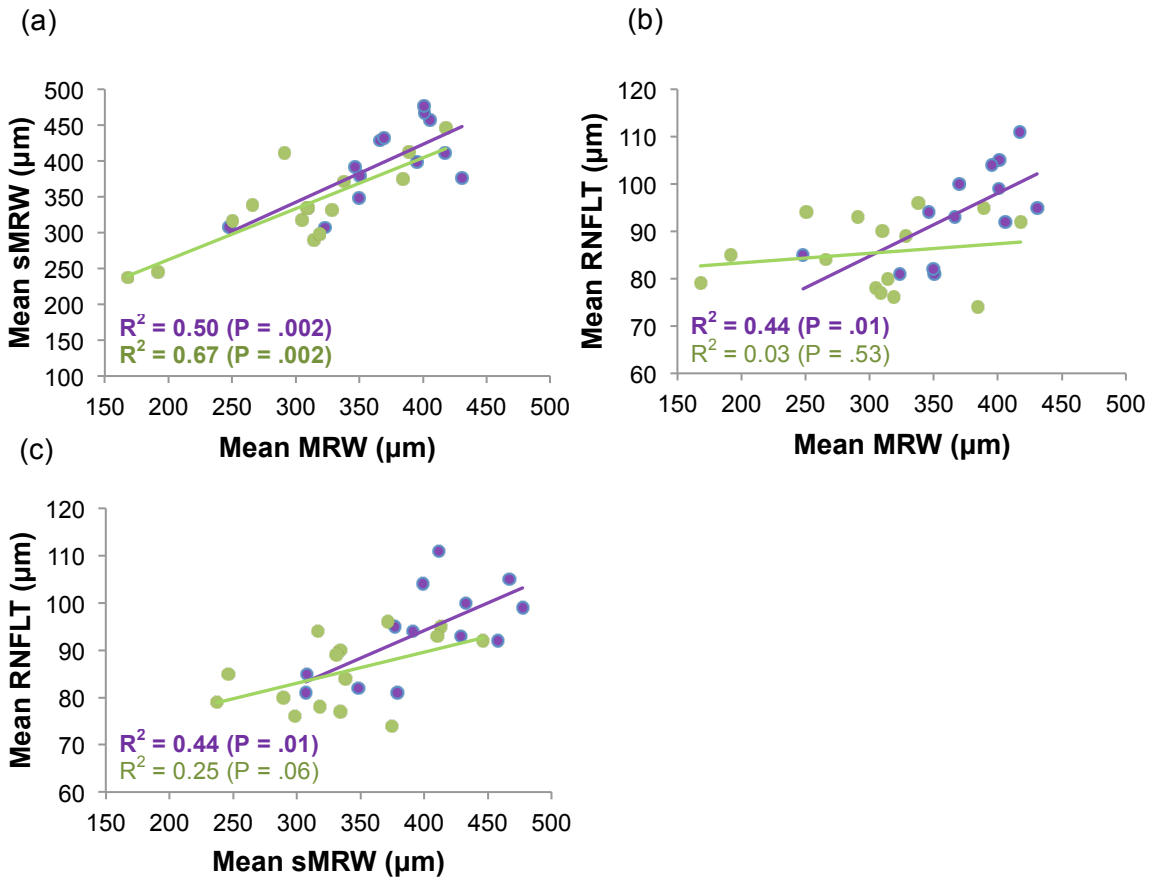

Figure 2-15. Comparison of ONH parameters plotted as a function of (a,b) mean MRW and (c) mean sMRW between young normal eyes with high myopia (purple circles) and older normal eyes with high myopia (green circles). Solid lines indicate linear regressions fit to the corresponding data points. P values were adjusted for multiple comparisons. (a) Mean sMRW was significantly correlated with mean MRW in young and older highly myopic eyes. (b) Mean RNFLT was significantly thicker in young highly myopic eyes that had thicker mean MRWs (*P*=.01) and (c) thicker mean sMRWs (*P*=.01).

2.4 Discussion

The purposes of this study were to better understand whether differences exist in ONH structure and ALCS position in (1) normal older eyes with varying levels of myopia and (2) in normal highly myopic eyes of different ages (i.e., young vs. older eyes). Measures of ONH and lamina cribrosa parameters were calculated from *in vivo* SDOCT images of the peripapillary retina and ONH acquired in eyes of normal older emmetropes/low myopes and normal older high myopes, as well as normal young high myopes. Most measured parameters were not significantly different between groups, with the exception of axon-related parameters (mean RNFLT when comparing older emmetropes/low myopes and older high myopes; mean MRW, sMRW and RNFLT when comparing young and older high myopes).

Subjects were intentionally classified as having emmetropia, low myopia or high myopia according to their refractive error (as opposed to axial length) since myopia is often categorized by refractive error in clinical settings. Refractive error is more accessible to clinicians, as additional instrumentation is required to measure axial length. Despite our use of refractive error as the criterion for classifying patients, we found a strong linear relationship between refractive error and axial length across all normal older eyes (Fig. 2-4f). Older eyes with increased axial lengths (longer eyes) tended to also have higher levels of myopia, as shown in previous studies (Hashemi, 2013).

Because myopia is a potential risk factor for the development and progression of glaucoma (Perkins and Phelps, 1982; Mitchell et al., 1999; Xu et al., 2007; Quigley, 2011), we examined whether differences exist in ONH and lamina cribrosa structure with axial length in older normal eyes. When analyzing all older eyes together, the only analyzed parameter that was significantly related to axial length was mean RNFLT (Fig. 2-4e). Similar to previous studies, we found that longer eyes tended to have thinner RNFLs (Savini et al., 2012; Nagai-Kushara et al., 2008; Rauscher et al., 2009; Budenz et

al., 2007). In addition, mean RNFLT was significantly thinner in our group of older highly myopic eyes relative to our older emmetropic/low myopic group (Table 2-1). These results are likely due to the fact that the circular scan used to measure RNFLT is performed over a fixed *angular* field size (12°) that will land at different physical distances from the ONH rim margin in eyes of different axial lengths. A fixed angular scan would be expected to sample a portion of retina that is located further from the ONH rim in an eye with a longer axial length where the RNFL will be anatomically thinner (i.e., decreased mean RNFLT) compared to an eye with a shorter axial length in which the scan would sample a location closer to the rim where the RNFL is known to be thicker (i.e., increased mean RNFLT). Patel et al. (2011) confirmed the idea that the significant correlation observed between RNFLT and axial length is due to differences in the retinal location sampled by the circular scan (relative to the ONH rim). After laterally scaling SDOCT images in 40 normal monkey eyes to account for magnification differences due to each eye's axial length and measuring RNFLT at a fixed physical distance from the ONH rim (as opposed to a fixed angular field size at different distances from the rim), Patel et al. (2011) found no significant relationship between RNFLT and axial length across subjects. This result implies that the significant relationship found between RNFLT and axial length in our older eyes would likely disappear after scaling RNFLT values for each eye's axial length. Interestingly, the significant linear relationship that was observed in our study between mean RNFLT and axial length when analyzing all older eyes together (Fig. 2-4e) was not seen within the older highly myopic group or within the older emmetropic/low myopic group (Fig. 2-8e). It is currently not clear why this relationship was more robust when analyzing all older eyes together.

When comparing ONH parameters in older eyes, our data suggest that the total number of axons in a human eye may be independent of the size of its ONH. While not statistically significant, mean MRW tended to be thinner in older normal eyes with larger

BMO areas (*P*=.12, Fig. 2-5b). However, as shown in Fig. 2-9b, mean MRW was found to significantly decrease (thin) with increasing BMO area (larger BMO) in our group of older highly myopic eyes (*P*=.04) (but not in our group of older emmetropes/low myopes). These results could imply that eyes with smaller BMOs might have more axons than eyes with larger BMOs (as MRW is thought to primarily consist of ganglion cell axon bundles). However, an alternative explanation could be that all eyes have a similar number of axons that can spread out more in eyes with larger BMO areas or stack more on top of each other in eyes with smaller BMO areas in order to exit through the neural canal (Fig. 2-16). Support for this latter possible explanation may come from our finding that there was no significant relationship between the scaled version of MRW (mean sMRW) and BMO area across our older highly myopic eyes (Fig. 2-9c). The disappearance of a significant relationship after scaling MRW to account for the individual variability in BMO circumference inherent across eyes could suggest that the number of axons is relatively similar in the highly myopic eyes despite differences in BMO area. While this concept conflicts with results from earlier studies reporting increased axon counts in human and non-human primate eyes with larger optic disk sizes (Quigley et al., 1991; Jonas et al., 1992), it may be supported by *ex vivo* histological studies that show axonal counts to be relatively similar (standard deviations <10% of total counts) within single species of non-human primate eyes (Perry and Cowey, 1985; Silveira et al., 1989; Fischer and Kirby, 1991; Herbin et al., 1997) and *in vivo* measures showing no significant relationships between mean sMRW and BMO area in a population of young normal subjects (Bhakta et al., 2016).

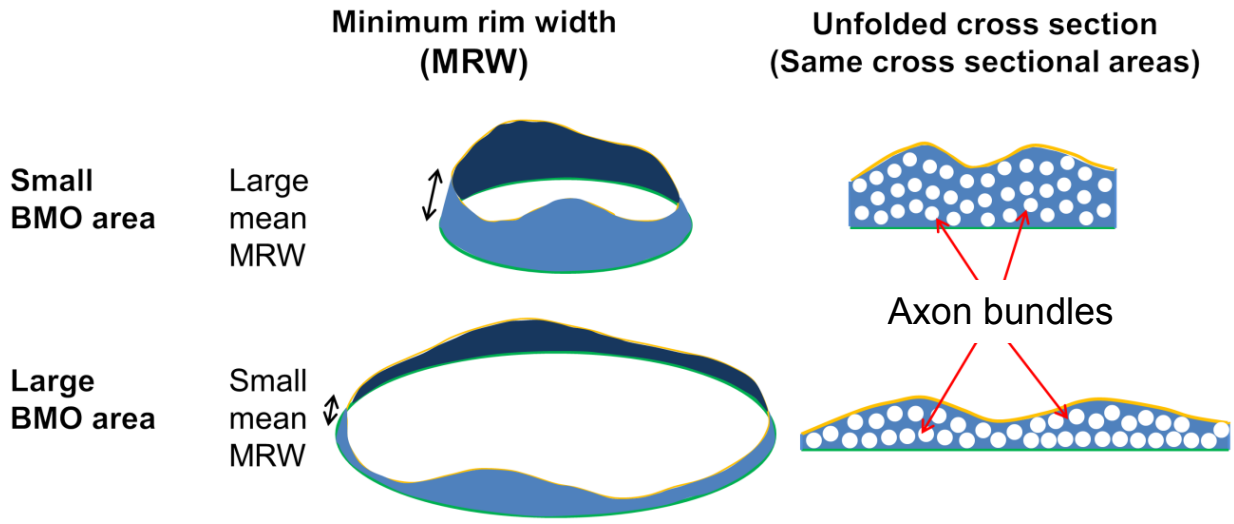

Figure 2-16. Illustration showing how similar numbers of axon bundles may possibly stack to yield larger MRWs in eyes with small BMO areas (top) or spread out to yield thinner MRWs in eyes with large BMO areas (bottom). Mean MRW (shaded in blue) is calculated as the mean perpendicular distance between the BMO ellipse (bottom green line) and inner limiting membrane (top yellow line) around the entire ONH. While mean MRW tended to be inversely correlated with BMO area in older normal eyes and older highly myopic eyes (i.e., eyes with smaller BMO areas had thicker MRWs [top left drawing] and eyes with larger BMO areas had thinner MRWs [bottom left drawing]), there was no significant relationship between these parameters after scaling mean MRW in every eye by the size of its BMO. In combination with previous studies, such a result could support the idea that eyes with different size BMOs could contain similar numbers of axon bundles (white circles in right-most pictures). (Right-most images) Assuming similar numbers of axon bundles, axons exiting the ONH would be forced to stack more (larger MRW) in an eye with a small BMO area than in an eye with a larger BMO area.

In addition to finding mean MRW to be significantly thinner in older highly myopic eyes with larger BMO areas, we also found a trend for mean MRW to be thinner in the same group of older highly myopic eyes who possessed larger mean ALCSDs (or more posteriorly-located anterior lamina cribrosa surfaces, ALCS's) (Fig. 2-10a). However, unlike the result with BMO area, MRW was nearly significantly correlated with mean ALCSD after scaling for each eye's BMO circumference (P=.06). As shown in Fig. 2-10b, older highly myopic eyes with larger mean ALCSD's also tended to have thinner mean sMRWs, potentially indicating that axons may be pulled more tautly to the BMO in older highly myopic eyes with a deeper lamina cribrosa. These possible tendencies for axons to be (1) more spread out in eyes with larger BMO areas and (2) pulled closer to the BMO in eyes with more posteriorly-located ALCS's could increase the biomechanical susceptibility of the older highly myopic eye to glaucomatous axonal damage due to increases in intraocular pressure that would likely push axons closer to the BMO and push the lamina cribrosa more posteriorly, exerting even more force on axons that are already taut and thinly distributed.

Given that age is a well-documented risk factor for the development of glaucoma (Gordon et al., 2002; Leske et al., 2003), we performed a secondary analysis to examine whether differences exist in ONH and lamina cribrosa structure with age in normal highly myopic eyes. The more myopic eye was selected for examination from 15 normal older and 13 normal younger human subjects with high myopia. Of all analyzed parameters, only axon-related quantities were significantly different between the 2 groups. Mean MRW, mean sMRW and mean RNFLT were all significantly thicker in young high myopic eyes than in older high myopic eyes. These findings (i.e., larger axonal content in younger eyes than in older eyes) are consistent with previous studies that have documented tendencies for axon counts to decrease with age (Harwerth and Wheat, 2008; Patel et al., 2014). Given that the RNFL and MRW are likely composed primarily

of ganglion cell axons, it is possible that our younger highly myopic eyes have elevated values of mean MRW, sMRW and RNFLT due to having larger numbers of axons compared to older highly myopic eyes (with potentially fewer numbers of axons).

Even though mean MRW samples all retinal ganglion cell axons, it's accuracy and meaning can potentially be enhanced through a metric that also incorporates the size of each eye's BMO. In this study, we chose to scale MRW thickness by multiplying the calculated value of mean MRW by the ratio of an individual eye's BMO circumference to the mean BMO circumference of a normal population (Patel et al., 2014). An alternative measurement that could provide improved understanding of the axonal content inherent in the thickness of the MRW is minimum rim area (MRA). Recently proposed by Gardiner et al. (2014), MRA is calculated by adding the areas of 48 trapeziums (one trapezium on each side of the ONH in all 24 radial B-scans), each of which extend from BMO delineated points to the ILM. Although there was no significant difference between the ability for MRA or MRW to predict RNFL thickness and mean deviation in their tested subjects, it would be valuable for future studies to assess both parameters in different populations and better understand whether sMRW and MRA provide similar or complimentary information detailing the impact of BMO size on MRW.

There were limitations associated with this study. One potential short-coming is that the number of subjects may not have been robust to detect whether differences may actually exist between our young and older highly myopic groups (n=13 and 15 subjects, respectively). For example, while not statistically significantly different, it is interesting to note that mean ALCSD was approximately 30 μm smaller (i.e. more anteriorly-located) in young high myopes compared to older high myopes (Table 2-2). If this observation were to become statistically significant and be confirmed in a larger cohort of eyes, it could potentially suggest that the ALCS migrates more posteriorly in highly myopic eyes during the normal aging process, mirroring changes typically measured in ALCS position in

early glaucoma (Bellezza et al., 2003; Strouthidis et al., 2011; He et al., 2014; Ivers et al., 2015). In addition, we placed no inclusion/exclusion criteria on the race or ethnicity of our subjects. Future studies could examine low and highly myopic populations that are more focused in the racial make-up, as it is well-established that race can play a role in ONH geometry (e.g., African-Americans typically have larger disk sizes than Caucasian individuals) (Dandona et al., 1990; Girkin et al. 2004; Girkin et al., 2011; Knight et al., 2012; Rhodes et al., 2014).

In conclusion, with the exception of mean RNFLT, there were no significant differences in analyzed ONH parameters between our older emmetropic/low myopic and highly myopic eyes. The fact that mean MRW was significantly thinner in older highly myopic eyes with larger BMO areas and tended to be thinner in these same eyes with more posteriorly-located ALCS's could indicate that axons are spread out and pulled more tautly toward the BMO in older highly myopic eyes with a deeper lamina, potentially placing their axons in a more susceptible position to suffer damage from increased levels of IOP. In addition, while ONH parameters were not significantly different between young and older highly myopic eyes, axon-related parameters were significantly thinner in the older eyes (likely reflecting age-related losses known to occur in normal eyes). The results from this study can serve as the basis of a normative database for comparison with future measurements of these parameters in older high myopes with different stages of glaucomatous progression.

2.5 Acknowledgements

This research was supported by NIH grants R01 EY021783 (JP), K23 EY021761 (NBP), T35 EY007088 (LJ Frishman), and P30 EY007551 (LJ Frishman) and the University of Houston College of Optometry. The authors thank Lisa Ostrin, Katrina Parker, Julianne

Knowles, Julia Benoit and Nripun Sredar for their assistance in patient recruitment and helpful discussions.

CHAPTER 3

General Conclusions

3.1 General Conclusions

Several structural changes occur in the retina, optic nerve head (ONH) and lamina cribrosa during glaucoma. Retinal nerve fiber layer thickness (RNFLT) in the circumpapillary region is a primary, objective clinical measurement used in the diagnosis of glaucoma. However, recent *in vivo* work in experimental models of glaucoma has shown that changes in the position of the anterior surface of the lamina cribrosa (or anterior lamina cribrosa surface depth, ALCSD) and in minimum rim width (MRW) can precede the earliest changes measured in RNFLT and potentially be earlier structural biomarkers of disease onset (Strouthidis et al., 2011; He et al., 2014; Patel et al., 2014). Given the emergence of these parameters as possible predictors of disease, it was important to understand their variability in normal eyes, as well as their relationships with each other and with risk factors for disease (such as high myopia and increased age). This study first examined whether there were differences in ONH structure between normal older subjects with low and high levels of myopia. As a secondary study relationships of ONH and retinal parameters were examined and compared between normal young high myopes and normal older high myopes.

Across all older normal myopic eyes, mean RNFLT was thinner in eyes with increased axial length (as previously known). When separated by refractive error (emmetropia/low myopia vs high myopia), however, this relationship was no longer present. Additionally, mean MRW was inversely correlated with BMO area across older highly myopic subjects, as older highly myopic eyes with larger BMO areas tended to have thinner mean MRWs. Yet, upon scaling MRW (sMRW) for each individual eye by taking into consideration the size of each eye's BMO, the same inverse correlation between BMO area and mean sMRW was not found. This result could imply that the number of axons in older highly myopic eyes is relatively constant regardless of the size of the BMO. To improve accuracy, the size of the BMO should be included when

accounting for changes in MRW thickness, either in the form of sMRW or perhaps with a newer method of calculating minimum rim area (MRA). Finally, the tendency for mean MRW to be thinner in older highly myopic eyes with more posteriorly-located ALCS's may indicate that axons are pulled more tautly toward the BMO in eyes with a deeper lamina. When coupled with the fact that mean MRW is also thinner in older highly myopic eyes with larger BMO areas, these findings may suggest that the ONH in normal older highly myopic eyes may be more anatomically susceptible to glaucomatous damage.

Following a comparison between emmetropic/low myopic and highly myopic older eyes, an evaluation of ONH structure was also made between younger high myopes and older high myopes. Mean RNFLT, MRW and sMRW were significantly thicker in younger highly myopic eyes than in older highly myopic eyes. It is likely that the larger numbers of axons inherent in younger myopic eyes (compared to older myopic eyes) are responsible for their elevated values of axon-related ONH parameters.

The results of this study have helped to define relationships of ONH parameters in older normal eyes with varying levels of myopia, and have provided insights into the role that high myopia may play in the development of ONH structure in younger and older eyes. The results serve as normative data for a population demographic not represented in SDOCT normative databases for glaucoma diagnostic equipment.

3.2 Summary and Future Directions

The introduction of high-resolution SDOCT imaging has provided the opportunity to better assess and understand the structural variability of ONH morphology in living human eyes. It can be used to better determine the impact that normal aging and higher levels of myopia may have on these structures. The findings of this thesis have helped to shed light on normative anatomical structure changes in multiple groups of subjects that

are at higher susceptibility for glaucomatous damage due to the inherent risk factors of high refractive error and older age. While ALCSD and MRW have been breakthrough measurement parameters in identifying earlier structural biomarkers of disease onset, other parameters (such as MRA) are worth investigating in an effort to better characterize the earliest time points of structural loss to facilitate earlier diagnosis and enable more informed clinical decision making in patients with higher risk of disease development. In addition, this study could be extended to examine whether differences exist in lamina cribrosa microarchitecture in eyes of different refractive errors using adaptive optics or swept source OCT imaging techniques. Finally, it will also be beneficial to pursue future studies that investigate the degree to which the results found within this study may depend on an individual's racial or ethic group.

REFERENCES

Bellezza AJ, Rintalan CJ, Thompson HW. Deformation of the lamina cribrosa and anterior scleral canal wall in early experimental glaucoma. *Invest Opthalmol Vis Sci*. 2003; 44: 623-637.

Bhakta AS, Sredar N, Marrelli D, Queener HM, Porter J. In vivo examination of lamina cribrosa microarchitecture and optic nerve head morphology in normal human eyes with age. *Invest Ophthalmol Vis Sci*. 2014; 55: 897.

Bhakta AS. In vivo examination of lamina cribrosa microarchitecture and optic nerve head geometry in normal human aging and early glaucoma (*Doctoral Dissertation*). 2016. University of Houston.

Budenz DL, Anderson DR, Varma R, et al. Determinants of Normal Retinal Nerve Fiver Layer Thickness Measured by Stratus OCT. *Ophthalmology*. 2007; 114:1046-1052.

Burgoyne CF, Downs JC, Bellezza AJ, Hart RT. Three-dimensional reconstruction of normal and early glaucoma monkey optic nerve head connective tissues. *Invest Ophthalmol Vis Sci*. 2004; 45: 4388-4399.

Carney L, Mainstone J, Henderson B. Corneal topography and myopia: A cross-sectional study. *Invest Ophthalmol Vis Sci*. 1997; 38: 311-320.

Chauhan BC, Danthurebandara VM, Sharpe GP. Bruch's membrane opening-minimum rim width and retinal nerve fiber layer thickness is a normal white population. A multi-center study. *Ophthalmology*. 2015; 122: 1786-1794.

Cheng H, Singh O, Kwong K, et al. Shape of the myopic eye as seen with high-resolution magnetic resonance imaging. *Optom Vis Sci*. 1992; 69: 698-670.

Curcio CA, Johnson M. Structure, function, and pathology of Bruch's membrane. In: Ryan SJ, Sadda SR, Hinton DR, Schachat AP, Sadda SR, Wilkinson CP, Wiedemann P, Schachat AP, eds. *Retina (5th ed.)*. London: WB Saunders; 2013, pp. 465-476.

Curtin BJ, Karlin DB. Axial length measurements and fundus changes of the myopic eye. *Am. J. Ophthalmol*. 1971; 71:42-53.

Dandona L, Quigley HA, Brown AE, Enger C. Quantitative regional structure of the normal human lamina cribrosa. A racial comparison. *Arch Ophthalmol*. 1990; 108: 393-398.

Dirani M, Chamberlain M, Shekar SN, Islam AF, Garoufalis P. Heritability of refractive error and ocular biometrics: the Genes in Myopia (GEM) twin study. *Invest Ophthalmol Vis Sci*. 2006; 47: 4756-4761.

Dirani M, Shekar SN, Baird PN. The role of educational attainment in refraction: the Genes in Myopia (GEM) twin study. *Invest Ophthalmol Vis Sci*. 2008; 49: 534-538.

Fischer QS, Kirby MA, Number and distribution of retinal ganglion cells in anubis baboons (Papio anubis). *Brain Behav Evol.* 1991; 37: 189-203.

Flanagan JG, Lonsberry B. The Optic Never and Glaucoma. *Optom Vis Sci*. 2013; 90: E-abstract GL-03.

Friedman DS, Wolfs RC, O'Colmain BJ, et al. Prevalence of open-angle glaucoma among adults in the United States. *Arch Ophthalmol*. 2004; 122: 532-538.

Gardiner SK, Ren R, Yang H, et al. A method to estimate the amount of neuroretinal rim tissue in glaucoma: Comparison with current methods for measuring rim area. *Am J Ophthalmol*. 2014; 157: 540-549.

Girkin CA, McGwin G Jr, Long C, et al. Subjective and objective optic nerve assessment in African Americans and whites. *Invest Ophthalmol Vis Sci*. 2004; 45: 2272-2278.

Girkin CA, McGwin G Jr, Sinai MJ, et al. Variation in optic nerve and macular structure with age and race with spectral-domain optical coherence tomography. *Ophthalmology*. 2011; 118: 2403-2408.

Gordon MO, Beiser JA, Brandt JD. The Ocular Hypertension Treatment Study: baseline factors that predict the onset of primary open-angle glaucoma. *Arch Ophthalmol*. 2002; 120: 714-720.

Gordon RA, Donzis PB. Refractive development of the human eye. *Arch Ophthalmol* 1985; 103: 785–789.

Goss DA, Grosvenor TP, Keller JT et al. Optometric Clinical Practice Guideline: Care of the patient with myopia. American Optometric Association. 1997.

Grosvenor T, Scott R. Role of axial length/corneal radius ratio is determining the refractive state of the eye. *Optom Vis Sci*. 1994; 71: 573-579.

Hammond CJ, Sneider H, Gilbert CE, Spector TD. Genes and environment in refractive error: the twin eye study. *Invest Ophthalmol Vis Sci.* 2001; 42: 1232-1236.

He L, Yang H, Gardiner SK, et al. Longitudinal detection of optic nerve head changes by spectral domain optical coherence tomography in early experimental glaucoma. *Invest Ophthalmol Vis Sci*. 2014; 55: 574-586.

Herbin M, Boire D, Ptito M. Size and distribution of retinal ganglion cells in the St. Kitts green monkey (Cercopithecus aethiops sabeus). *J Comp Neurol.* 1997; 383: 459-472.

Huang D, Swanson EA, Lin CP. Optical Coherence Tomography. *Science*. 1994; 254: 1178-1181.

Ivers KM, Li C, Patel N, et al. Reproducibility of measuring lamina cribrosa pore geometry in human and nonhuman primates with in vivo adaptive optics imaging. *Invest Ophthalmol Vis Sci.* 2011; 52: 5473-5480.

Ivers KM, Sredar N, Patel NB, et al. In vivo changes in lamina cribrosa microarchitecture and optic nerve head structure in early experimental glaucoma. *PLoS ONE* 2015; 10:e0134223.

Jonas JB, Berenshtein E, Holbach L. Anatomic relationship between lamina cribrosa, intraocular space, and cerebrospinal fluid space. *Invest Ophthalmol Vis Sci*. 2003; 44(12):5189-5195.

Jonas JB, Gusek GC, Naumann GO. Optic disk morphometry in high myopia. Graefe's archive for clinical and experimental ophthalmology. *Albrecht von Graefes Archiv fur klinische und experimentelle Ophthalmologie*. 1988; 226: 587-590.

Kempen JH, Mitchell P, Lee KE, Tielsch JM, Broman AT. The prevalence of refractive errors among adults in the United States, Western Europe, and Australia. *Arch Ophthalmol.* 2004; 122: 495-505.

Klein RM, Curtin BJ. Lacquer crack lesions in pathologic myopia. *Am. J. Ophthalmol*. 1979; 79: 386-392.

Knight OJ, Girkin CA, Budenz DL, Durbin MK, Feuer WJ. Effect of race, age, and axial length on optic nerve head parameters and retinal nerve fiber layer thickness measured by Cirrus HD-OCT. *Arch Ophthalmol.* 2012; 130: 312-318.

Leske MC, Connell AM, Wu SY, Hymen LG, Schachat AP. Risk factors for open-angle glaucoma. The Barbados Eye Study. *Arch Ophthalmol*. 1995; 113: 918-924.

Leske MC, Heijl A, Hussein M, et al. Factors for glaucoma progression and the effect of treatment: the early manifest glaucoma trial. *Arch Ophthalmol*. 2003; 121: 48-56.

Li C, Sredar N, Ivers KM, Queener H, Porter J. A correction algorithm to simultaneously control dual deformable mirrors in a woofer-tweeter adaptive optics system. *Opt Express*. 2010; 18: 16671-16684.

Li YJ, Guggenheim JA, Bulusu A, Metlapally R, Abbott D. An international collaborative family-based whole-genome linkage scan for high-grade myopia. *Invest Ophthalmol Vis Sci.* 2009; 50: 3116-3127.

Mainstone J, Carney L, Anderson C, et al. Corneal shape in hyperopia. *Clin Exp Optom*. 1998; 81: 131-137.

Malakar M, Askari SN, Ashraf H. Optical coherence tomography assisted retinal nerve fibre layer thickness profile in high myopia. *J Clin Diagn Res.* 2015; 9, NC01-03.

Mitchell P, Hourihan F, Sandbach J, Wang JJ. The relationship between glaucoma and myopia: The Blue Mountains Eye Study. *Ophthalmology*. 1999; 106: 2010-2015.

Nagai-Kusuhara A, Nakamuru M, Fujioka M, et al. Association of retinal nerve fibre layer thickness measured by confocal scanning laser ophthalmoscopy and optical coherence tomography with disc size and axial length. *Br J Ophthalmol*. 2008; 92:186-190.

Naidoo K, Govender P, Holden B. The uncorrected refractive error challenge. *Community Eye Health.* 2014; 27: 74-75.

Oliveira C, Harizman N, Girkin CA, et al. Axial length and optic disc size in normal eyes. *Br J Ophthalmol*. 2007; 91: 37-39.

Pascolini D, Mariotti SP. Global estimates of visual impairment: 2010. *Br J Ophthalmol*. 2012; 96: 614-618.

Patel NB, Luo X, Wheat JL, Harwerth RS. Retinal nerve fiber layer assessment: Area versus thickness measurements from elliptical scans centered on the optic nerve. *Invest Ophthalmol Vis Sci*. 2011; 52: 2477-2489.

Patel NB, Sullivan-Mee M, Harwerth RS. The relationship between retinal nerve fiber layer thickness and optic nerve head neuroretinal rim tissue in glaucoma. *Invest Ophthalmol Vis Sci*. 2014; 55: 6802-6816.

Perkins ES, Phelps CD. Open angle glaucoma, ocular hypertension, low-tension glaucoma, and refraction. *Arch Ophthalmol*. 1982; 100: 1464-1467.

Perry VH, Cowey A. The ganglion cell and cone distributions in the monkey's retina: implications for central magnification factors. *Vision Res.* 1985; 25: 1795-1810.

Quigley HA, Addicks EM. Regional differences in the structure of the lamina cribrosa and their relation to glaucomatous optic nerve damage. *Arch Ophthalmol*. 1981; 99: 137-143.

Quigley HA, Coleman AL, Dorman-Pease ME. Larger optic nerve heads have more nerve fibers in normal monkey eyes. *Arch Ophthalmol*. 1991; 109: 1441-1443.

Quigley HA. Number of people with glaucoma worldwide. *Br J Ophthalmol*. 1996; 80: 389-393.

Quigley HA. Glaucoma. *Lancet*. 2011; 377: 1367-1377.

Rauscher FM, Sekhon N, Feuer WJ, Budenz DL. Myopia affects Retinal Nerve Fiber Layer Measurements as Determined by Optical Coherence Tomography. *J Glaucoma*. 2009; 18(7): 501-505.

Ren R, O'Leary N, Yang H, et al. Influence of clinically invisible, but optical coherence tomography detected, optic disc margin anatomy on neuroretinal rim evaluation. *Invest Ophthalmol Vis Sci*. 2012; 53: 1852-1860.

Rhodes LA, Huisingh C, Johnstone J, et al. Variation of laminar depth in normal eyes with age and race. *Invest Ophthalmol Vis Sci*. 2014; 55: 8123-8133.

Savini G, Bardoni P, Vincenzo P, Carbonelli M. The influence of axial length on retinal nerve fibre layer thickness and optic-disc size measurements by spectral domain OCT. *Br J Ophthalmol*. 2012; 96:57-61.

Silveira LC, Picanco-Diniz CW, Sampaio LF, Oswaldo-Cruz E. Retinal ganglion cell distribution in the cebus monkey: a comparison with the cortical magnification factors. *Vision Res*. 1989; 29: 1471-1483.

Sperduto RD, Seigel D, Roberts J, Rowland M. Prevalence of myopia in the United States. *Arch Ophthalmol*. 1983; 101: 405-407.

Sredar N, Ivers KM, Queener H, Zouridakis G, Porter J. 3D modeling to characterize lamina cribrosa surgace and pore geometries using in vivo images from normal and glaucomatous eyes. *Biomed Opt Express*. 2013; 4: 1153-1165.

Strang N, Schmid K, Carney L. Hyperopia is predominantly axial in nature. *Curr Eye Res*. 1998; 17: 380-383.

Strouthidis NG, Fortune B, Yang H, Sigal IA, Burgoyne CF. Longitudinal change detected by spectral domain optical coherence tomography in the optic nerve head and peripapillary retina in experimental glaucoma. *Invest Ophthalmol Vis Sci*. 2011; 52: 1206-1219.

Tham YC, Li X, Wong TY, Quigley HA, Aung T, Cheng CY. Global prevalence of glaucoma and projections of glaucoma burden through 2040: a systematic review and meta-analysis. *Ophthalmology*. 2014; 121: 2081-2090.

Tron EJ. The optical elements of the refractive power of the eye. In: Ridley F, Sorsby A, eds. *Modern Trends in Ophthalmology*. New York; Paul B. Hoeber; 1940; 245-255.

Wong TY, Klein BE, Klein R, Knudtson M, Lee KE. Refractive errors, intraocular pressure, and glaucoma in a white population. *Ophthalmology*. 2003; 110: 211-217.

Xu L, Wang Y, Wang S, Jones JB. High myopia and glaucoma susceptibility: The Beijing Eye Study. *Ophthalmol*. 2007; 114: 216-220.

Yang H, Ren R, Lockwood H. The connective tissue components of optic nerve head cupping in monkey experimental glaucoma part 1: Global change. *Invest Ophthalmol Vis Sci*. 2015; 56: 7661-7678.